

**PREPARATION OF NANOCOMPOSITE MATERIALS FOR  
PHOTOCATALYTIC WATER TREATMENT**

**A THESIS SUBMITTED TO  
THE GRADUATE SCHOOL OF NATURAL AND APPLIED SCIENCES  
OF  
ATILIM UNIVERSITY**

**BY**

**NAWAR RAZZAQ KADHIM SALIHI**

**IN PARTIAL FULFILLMENT OF THE REQUIREMENTS FOR THE  
DEGREE OF MASTER OF SCIENCE**

**IN**

**APPLIED CHEMISTRY**

**AT**

**THE DEPARTMENT OF CHEMICAL ENGINEERING AND  
APPLIED CHEMISTRY**

**OCTOBER 2017**

Approval of the Graduate School of Natural and Applied Sciences, Atılım University.

---

Prof. Dr. Ali KARA

Director

I certify that this thesis satisfies all the requirements as a thesis for the degree of Master of Science.

---

Prof. Dr. Atilla CİHANER

Head of Department

This is to certify that we have read the thesis “Preparation of Nanocomposite Materials for Photocatalytic Water Treatment” submitted by “Nawar Razzaq Kadhim Salihi” and that in our opinion it is fully adequate, in scope and quality, as a thesis for the degree of Master of Science.

---

Assoc. Prof. Dr. Murat KAYA

Supervisor

Examining Committee Members

Assoc. Prof. Dr. Seha TİRKEŞ

Asst. Prof. Dr. Ferdi KARADAŞ

Assoc. Prof. Dr. Murat KAYA

Date: 13.10.2017

I declare and guarantee that all data, knowledge and information in this document has been obtained, processed and presented in accordance with academic rules and ethical conduct. Based on these rules and conduct, I have fully cited and referenced all material and results that are not original to this work.

Name, Last name: Nawar Razzaq Kadhim Salihi

Signature:

## **ABSTRACT**

### **PREPARATION OF NANOCOMPOSITE MATERIALS FOR PHOTOCATALYTIC WATER TREATMENT**

SALIHI, Nawar Razzaq Kadhim

M.Sc., Chemical Engineering and Applied Chemistry

Supervisor: Assoc. Prof. Dr. Murat KAYA

October 2017, 54 pages

One of the crucial concerns is water resources and its related troubles have gained importance due to continuous pollution of ecological water systems. Nowadays, researchers are interested in the improved techniques that can provide the degradation of organic pollutants by oxidation. Consequently, semiconductor photocatalysis technology has prompted scientists to provide environmental remediation. Recently, within the semiconductor photocatalysts, especially ZnO has gained attention because of usage in the removal of industry based wastes in air and water. This photocatalyst can be used as treatment method because of proper qualities such as being low-cost, environmentally friendly, and sustainability.

Besides ZnO, there are a number of semiconductors that can be utilized for water pollution treatment; however, effective separation, recycling and dispersion are still important challenge for these tiny powdered photocatalyst. Magnetic property provides magnetic separation effectively and simply for removal of suspended catalyst particles from waste water without using any further separation techniques. The magnetic property also provides the suspension of photocatalyst that allows great surface area for catalytic reactions.

In this study, to obtain photocatalyst with high activity and well-separation quality, a facile procedure to fabricate magnetic cobalt ferrite ( $\text{SiO}_2\text{-CoFe}_2\text{O}_4$ ) and zinc oxide (ZnO) added PEDOT ( $\text{SiO}_2\text{-CoFe}_2\text{O}_4\text{/PEDOT/ZnO}$ ) a novel magnetically recyclable nanocomposite material as a photocatalyst was demonstrated. Scanning electron microscopy (SEM), transmission electron microscopy (TEM), high resolution- transmission electron microscopy (HR-TEM) and energy dispersive X-Ray (EDX) were utilized for the characterization of nanocomposite photocatalysts. The photocatalytic activity of  $\text{SiO}_2\text{-CoFe}_2\text{O}_4\text{/PEDOT/ZnO}$  nanocomposite material was tested into the decolorisation of methylene blue (MB) under UV light irradiation. The photocatalytic activity of ZnO, PEDOT and ZnO/PEDOT was also shown to check the improvement compared to the final structure.

Consequently, the usage of PEDOT and the interaction of ZnO with this polymer synergetically improve the photocatalytic activity. In addition to high activity of the photocatalyst, the synthesized  $\text{SiO}_2\text{-CoFe}_2\text{O}_4\text{/PEDOT/ZnO}$  nanocomposite material has magnetic property as an advantage. PEDOT provides not only the improved activity of photocatalysis but also supplementation of magnetic nanoparticles that brings magnetic quality to the ultimate structure.

**Keywords:** Photocatalyst, ZnO nanoparticles, PEDOT, magnetic separation, waste water treatment

## ÖZ

### FOTOKATALİTİK SU ARITIMI İÇİN NANOKOMPOZİT MALZEME HAZIRLANMASI

SALIHI, Nawar Razzaq Kadhim

Yüksek Lisans, Kimya Mühendisliği ve Uygulamalı Kimya Bölümü

Tez Yöneticisi: Doç. Dr. Murat KAYA

Ekim 2017, 54 sayfa

Önemli sorunlardan biri olarak su kaynakları ve ilgili sıkıntılar, ekolojik su sistemlerinin sürekli olarak kirlenmesi nedeniyle önem kazanmıştır. Günümüzde, araştırmacılar organik kirleticilerin oksidasyon ile bozunmasını sağlayan gelişmiş tekniklerle ilgilenmektedirler. Sonuç olarak, yarı iletken fotokatalizör teknolojisi, bilim insanlarını çevresel ıslahın sağlanabilmesi için yönlendirmiştir. Son zamanlarda, yarı iletken fotokatalizörler içerisinde, özellikle ZnO, hava ve sudaki endüstri temelli atıkların gideriminde kullanılması nedeniyle ilgi çekmektedir. Bu fotokatalizör, düşük maliyeti, çevre dostu olması ve sürdürülebilirlik gibi uygun niteliklerinden dolayı arıtma yöntemi olarak kullanılabilir.

ZnO dışında, su kirliliği arıtması için kullanılabilecek pek çok yarı iletken bulunmaktadır, ancak bu küçük parçacıklı toz halindeki fotokatalizörler için, etkili ayırma, yeniden kullanım ve dağılım hala önemli problemlerdendir. Manyetik özellik, askıda kalan katalizör parçacıklarının atık sudan başka ayırma tekniklerine gerek duymadan uzaklaştırılması için manyetik ayırmanın etkili bir şekilde uygulanmasını sağlamaktadır. Manyetik özellik ayrıca fotokatalizörün sıvıda dağılımını sağlayarak katalitik reaksiyonlar için büyük yüzey alanının oluşmasına imkan verir.

Bu çalışmada, yüksek aktiviteye ve iyi ayrılma özelliğine sahip fotokatalizör elde etme amacıyla, manyetik kobalt ferrit ( $\text{SiO}_2\text{-CoFe}_2\text{O}_4$ ) ve çinko oksit ( $\text{ZnO}$ ) eklenmiş PEDOT ( $\text{SiO}_2\text{-CoFe}_2\text{O}_4/\text{PEDOT}/\text{ZnO}$ ) içeren manyetik olarak geri kazanımlı fotokatalizör olarak kullanılabilen yeni bir nanokompozit malzeme üretmek için basit bir yöntem gösterilmiştir. Taramalı elektron mikroskobu (SEM), geçirimsiz elektron mikroskobu (TEM), yüksek çözünürlüklü transmisyon elektron mikroskobu (HR-TEM), enerji dağılımlı X-ışını (EDX) nanokompozit fotokatalizörlerin karakterizasyonunda kullanılmıştır.  $\text{SiO}_2\text{-CoFe}_2\text{O}_4/\text{PEDOT}/\text{ZnO}$  nanokompozit malzemenin fotokatalitik aktivitesi metilen mavisinin (MB) UV ışık kaynağı altında renginin giderilmesi çalışması ile test edilmiştir.  $\text{ZnO}$ , PEDOT ve  $\text{ZnO}/\text{PEDOT}$ 'un fotokatalitik aktiviteleri son yapıdaki iyileştirmenin kontrol edilebilmesi için ayrıca gösterilmiştir.

Sonuç olarak, PEDOT polimer kullanımı ve  $\text{ZnO}$ 'in bu polimer ile sinerjik etkileşimi fotokatalitik aktiviteyi iyileştirmektedir. Fotokatalizörün yüksek aktivitesinin yanı sıra, sentezlenen  $\text{SiO}_2\text{-CoFe}_2\text{O}_4/\text{PEDOT}/\text{ZnO}$  nanokompozit malzeme avantaj olarak manyetik özelliğe de sahiptir. PEDOT fotokatalizörün aktivitesinde iyileşme sağlamanın yanı sıra, nanokompozit yapıya manyetik özellik kazandıran manyetik nanoparçacıkların ilave edilmesine olanak sağlamaktadır.

**Anahtar Kelimeler:** Fotokatalizör,  $\text{ZnO}$  nanoparçacıklar, PEDOT, manyetik ayırma, atık su arıtma



**To My Family**

## ACKNOWLEDGEMENTS

In the name of greatest All mighty ALLAH who has always bless us with potential knowledge and success.

This thesis marks the end of my MSc degree. I would not have been able to do so without the support and assistance of my supervisor Assoc. Prof. Dr.Murat Kaya I take this opportunity to extend my utmost gratitude to for his support and guidance towards my project. He was not only my supervisor but also my friends in my life. I owe great thanks to him.

I would also like to thank to Ceren Uzun for her support, advice and assistance every step of the way. She has given me so much motivation to work hard towards my goals. Thank you to all the members of the analytical Laboratory for all the assistance and support. I would like to extend my appreciation to all academic staffs in the Department of Chemical Engineering and Applied Chemistry at Atilim University for their efforts and helps.

Special thanks to my country for financial assistance.

Finally, and most importantly, I would like to thank my wife Safa Algraholi. Her support, encouragement, quiet patience and unwavering love were undeniably the bedrock upon which the past ten years of my life have been built. Her tolerance of my occasional vulgar moods is a testament in itself of her unyielding devotion and love.I thank my parents, Razzaq Alsalihi, for their faith in me and allowing me to be as ambitious as I wanted, and pray for me in life. To my children Yousif and Daniha, words cannot describe how grateful I am for all your sacrifices and patience.

This study was partially supported by TUBİTAK (115Z550).

## TABLE OF CONTENTS

ABSTRACT .....	iv
ÖZ .....	vi
ACKNOWLEDGEMENTS .....	ix
TABLE OF CONTENTS .....	x
LIST OF FIGURES .....	xii
LIST OF TABLES .....	xiv
CHAPTER 1 .....	1
INTRODUCTION .....	1
1.1    Advanced Oxidation Processes (AOP) .....	3
1.2    Heterogeneous Photocatalysis System .....	4
1.3    Photocatalytic Degradation of Organic Compounds Under Light Radiation .....	7
1.4    ZnO as a Photocatalytic Material .....	10
1.5    Conjugated Polymers for Photocatalysis .....	14
1.6    Separation Process of Photocatalysis .....	16
1.7    Aim of the Study .....	16
CHAPTER 2 .....	17
MATERIALS AND METHODS .....	17
2.1.    Materials .....	17
2.2.    Characterization and Instrumentation .....	17
2.3.    Preparation of Silica Coated Cobalt Ferrite (SiO <sub>2</sub> -CoFe <sub>2</sub> O <sub>4</sub> ) Magnetic Nanoparticles .....	18
2.4.    Preparation of PEDOT .....	20
2.5.    Preparation of PEDOT/ZnO and SiO <sub>2</sub> -CoFe <sub>2</sub> O <sub>4</sub> /PEDOT/ZnO Nanocomposite Material .....	20
2.6.    Determination of Catalytic Performance of the Prepared Materials	22

CHAPTER 3 .....	24
RESULTS AND DISCUSSION .....	24
3.1.    Preparation and Characterization of Magnetic Cobalt Ferrite Nanoparticles with Silica Shell .....	25
3.2.    Preparation and Characterization of Nanomaterials Prepared in This Study .....	27
3.3.    Magnetic Property of Prepared SiO <sub>2</sub> -CoFe <sub>2</sub> O <sub>4</sub> /PEDOT/ZnO Nanocomposite Material .....	31
3.4.    Photocatalytic Activity Studies of the Prepared Materials .....	32
3.4.1.  Adsorption-Desorption Profiles of the Prepared Nanostructures ..	33
3.4.2.  Photocatalytic Activity of the Prepared Nanostructures.....	33
CHAPTER 4 .....	41
CONCLUSION.....	41
REFERENCES.....	43

## LIST OF FIGURES

### FIGURES

Figure 1.1 The efficiency of photocatalysis technologies. <sup>3</sup> .....	5
Figure 1.2 The steps of the photocatalytic process, a) photoexcitation causes the formation of electron ( $e^-$ )–hole ( $h^+$ ) pairs; b) photoinduced charge recombination and photoinduced charge transportation, oxidation and reduction processes; c) formation of ions. <sup>3</sup> .....	6
Figure 2.1 The preparation procedure of $CoFe_2O_4$ magnetic nanoparticles. ....	19
Figure 2.2 Silica coating over $CoFe_2O_4$ nanoparticles.....	19
Figure 2.3 Preparation of PEDOT .....	20
Figure 2.4 Preparation of $SiO_2-CoFe_2O_4/PEDOT/ZnO$ nanocomposites. ....	21
Figure 2.5 Photocatalytic reactor used in this study .....	22
Figure 2.6 UV-Vis spectrophotometer used for decolorisation experiments.....	23
Figure 3.1 TEM image of the prepared $SiO_2-CoFe_2O_4$ magnetic nanoparticles.....	26
Figure 3.2 EDX patterns of $SiO_2-CoFe_2O_4$ magnetic nanoparticles.....	27
Figure 3.3 TEM image of ZnO nanoparticles. ....	28
Figure 3.4 EDX pattern of ZnO nanoparticles. ....	28
Figure 3.5 SEM image of PEDOT. ....	29
Figure 3.6 TEM image of $SiO_2-CoFe_2O_4/PEDOT/ZnO$ nanocomposite material. ....	30
Figure 3.7 EDX patterns of $SiO_2-CoFe_2O_4/PEDOT/ZnO$ nanocomposite material...	31
Figure 3.8 Magnetic behavior of $SiO_2-CoFe_2O_4/PEDOT/ZnO$ nanocomposite material under external magnetic field (1.6 T).....	31

Figure 3.9 Photocatalytic removal of methylene blue under UV light exposure by using 10 mg ZnO nanoparticles as catalyst.....	34
Figure 3.10 Photocatalytic removal of methylene blue under UV light exposure by using 10 mg PEDOT as catalyst.....	36
Figure 3.11 Photocatalytic removal of methylene blue under UV light exposure by using 10 mg PEDOT/ZnO nanocomposite material as catalyst. ....	37
Figure 3.12 Photocatalytic removal of methylene blue under UV light exposure by using 10 mg SiO <sub>2</sub> -CoFe <sub>2</sub> O <sub>4</sub> /PEDOT/ZnO nanocomposite material as catalyst.....	39



## LIST OF TABLES

### TABLES

Table 1.1 Advantages and disadvantages of chemical / physical methods.....	2
Table 3.1 Percent dye removal efficiency of ZnO nanoparticle under UV light exposure.....	34
Table 3.2 Percent dye removal efficiency of PEDOT polymer under UV light exposure.....	36
Table 3.3 Percent dye removal efficiency of PEDOT/ZnO nanocomposite material under UV light exposure.....	38
Table 3.4 Percent dye removal efficiency of SiO <sub>2</sub> -CoFe <sub>2</sub> O <sub>4</sub> /PEDOT/ZnO nanocomposite material under UV light exposure.....	39

## **CHAPTER 1**

### **INTRODUCTION**

Waste water based pollution through industry is the most widespread reason of environmental pollution. Industrial wastes consist of several toxic chemicals particularly synthetic dyes that are extremely carcinogen. Although the decomposition of dyes can be achieved aerobically and anaerobically, still these reactions causes the production of some compounds that are carcinogenic in nature. There are several conventional methods such as adsorption, chlorination, coagulation, ion flotation, membrane process, sedimentation and solvent extraction that are still utilized to purify waste water. Yet, these methods have side products that require further efforts to provide purification completely. The advantages and disadvantages of these conventional methods can be seen in Table 1.<sup>1,2,3</sup>

**Table 1.1** Advantages and disadvantages of chemical / physical methods. <sup>1,2,3</sup>

<b>Treatment methods</b>	<b>Advantages</b>	<b>Disadvantages</b>
Electrocoagulation/ coagulation	Cost-effective	Sludge production
Ozonation	Used in a gaseous state and therefore has no volume limitations	Has a short half-life - approximately 20 minutes
Filtration	Can be used universally for all dyes	Produces slurries
Biological methods	Environmentally friendly and cost-effective	May form by-products, require secondary treatment
Irradiation	Can be successfully applied at lab scale	Requires a large amount of dissolved oxygen
Ion-exchange	Stable adsorbent and has the ability to redevelop	Cannot effectively remove all dyes
Fenton's reagent	Effective decolourisation of all dyes	Sludge production
Activated Carbon	Applicable to a wide variety of dyes	Expensive
Silica gel	Removes basic dyes	Cannot be used for commercial use, due to side reaction

Novel oxidation processes are enhanced to break down the toxic pollutants to harmless carbon dioxide and water. These techniques consist of biodegradation, fenton, photofenton, photocatalytic radiation, sonolysis, ozonation, and UV photocatalysis. Although the mentioned enhanced oxidation processes are more effective than chemical techniques, these methods are relatively expensive. The developments in nanoscience as a novel branch of science has taken place of former technologies because of following reasons. Firstly, most of organic chemicals can be mineralized by nanomaterials, and these materials are relatively cheap. Secondly, semiconducting nanostructures can be utilized to get rid of organic pollutants totally from waste water. Thirdly, nanophotocatalysts are not poisonous, resistant to oxidation, not reactive chemically and thermally. Finally, photocatalysts are easily prepared, cheap and stable to oxidation when there is water and chemicals in the medium.

For the preparation of photocatalyst, various advanced nanostructures can be synthesized via varied processes. These photocatalysts have different application areas such as environmental remediation, sterilization, production of hydrogen and renewable energy. A nanophotocatalyst especially can be used in the treatment of toxic materials such as dyes that exist in industrial waste water. For environmental remediation, novel researches related with composition, surface area, shape, size and structure of nanophotocatalyst should be done to design enhanced photocatalyst for now and future.<sup>4</sup>

## **1.1 Advanced Oxidation Processes (AOP)**

Advanced Oxidation Processes (or Advanced Oxidative Technologies) interests in the novel technologies that is proper to minimize environmental influence to the living beings.<sup>5</sup> Of these technologies, the photocatalytic degradation of pollutants is the technique that is utilized particularly light radiation.<sup>6,7,8</sup> The photocatalysts in this technique are described as having ability to provide degradation of organic pollutants to carbondioxide, water and inorganic anions.

The degradation reactions are taking place through the reactions that consist of formation of oxidizing species, especially hydroxyl radicals with high oxidizing power ( $E_0=2.8$  V).<sup>8,9,10</sup> These processes consist of the usage of ozone, hydrogen peroxide, Fenton and photo-Fenton reactions that involve decomposition of hydrogen peroxide in acidic medium catalytically, and semiconductors as heterogenous photocatalyst.<sup>9,10</sup>

Of the advanced oxidation technologies, especially the heterogenous photocatalysis seems to satisfy expectations. Heterogenous photocatalytic processes consist of formation of extreme oxidizing reactive oxygen species such as hydroxyl and superoxide radicals as a result of interaction between the electronically excited semiconducting material, oxygenated species and other materials.<sup>8,10,11,12</sup>

## **1.2 Heterogeneous Photocatalysis System**

There is exclusive interest to semiconductor photocatalyst technology among scientists related with environmental remediation (Figure 1.1). Compared to other techniques, no further necessity for secondary removal method exists for this process. On the other hand, as the process is taking place at or near room temperature and pressure, it is conceivable as a kind of eco-friendly process.<sup>13</sup>

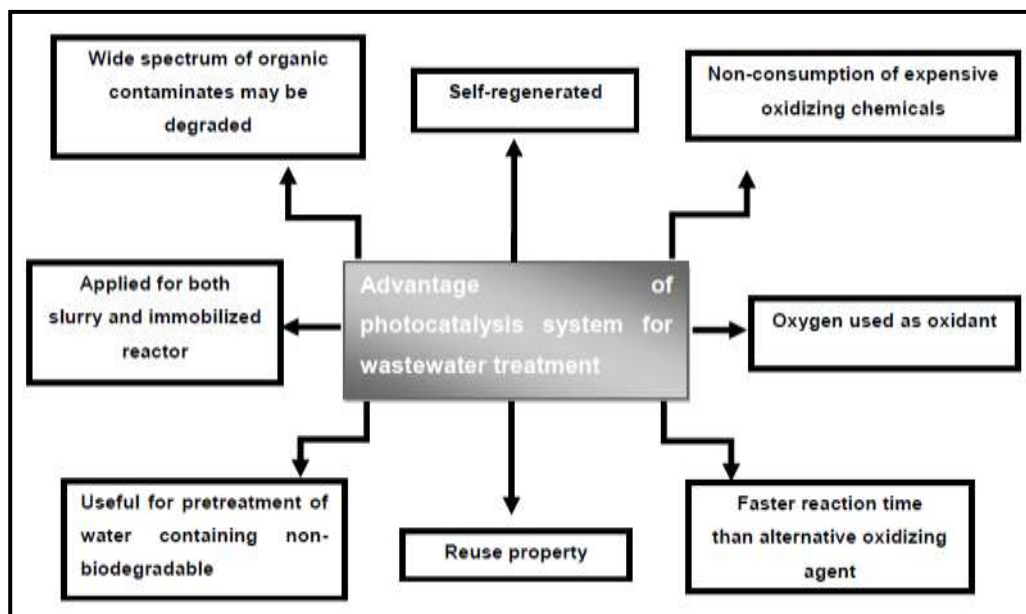


**Figure 1.1** The efficiency of photocatalysis technologies.<sup>3</sup>

Recently, photocatalysts consist of  $\text{TiO}_2$ ,  $\text{ZnO}$ , and  $\text{CdS}$  have gained great importance in the applications of deodorization, antimicrobial purification of air and water, treatment of waste water because, they have several advantages such as having high physical and chemical performances, being cheap, and available with high stability.<sup>14</sup> By photocatalysts, several organic materials can be oxidized, and finally turned to  $\text{CO}_2$ ,  $\text{H}_2\text{O}$ , and other safe products. Considering  $\text{ZnO}$  as an example of photocatalytic material, the mechanism of the process is shown in Figure 1.2.

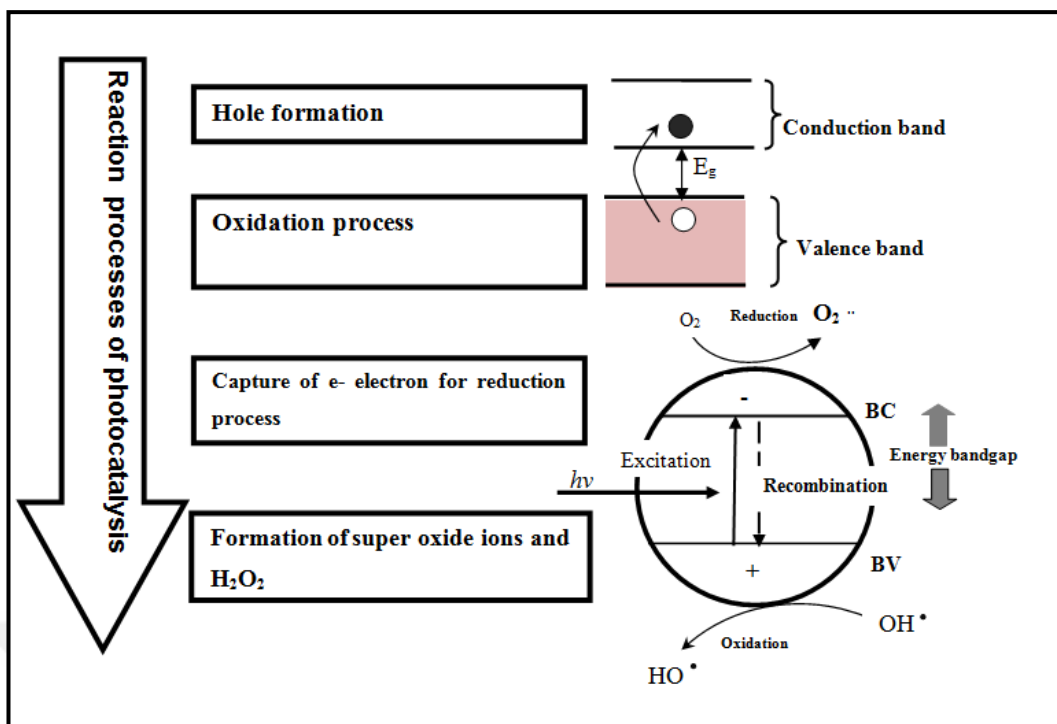


**Figure 1.2** The steps of the photocatalytic process, a) photoexcitation causes the formation of electron ( $e^-$ )–hole ( $h^+$ ) pairs; b) photoinduced charge recombination and photoinduced charge transportation, oxidation and reduction processes; c) formation of ions.<sup>3</sup>

The applications of heterogenous photocatalysis has been reported in the studies of Fujishima and Honda.<sup>15</sup> Activation of semiconductor by photon is related with its electronic excitation in which the energy of photons is greater than that of band gap energy of semiconducting material. This process is disposed to formation of vacancies in valence band-VB (holes,  $h^+$ ), and high electron density regions ( $e^-$ ) in conduction band-CB.<sup>8,9,16</sup> The formed holes with +2.0 and +3.5 V values have pH dependent and extremely positive electrochemical potentials which was measured with a saturated calomel electrode.<sup>17</sup>

This potential range is properly positive to provide formation of hydroxyl radicals (HO<sup>•</sup>) on the semiconducting material surface from water molecules adsorbed. The performance of photocatalyst is linked to competition among the formed electrons and holes on the surface of semiconducting material and recombination of them.<sup>5,8,18</sup> The electrons moved to conduction band provide several reducing reactions that consist of the production of gaseous hydrogen and the formation of crucial oxidizing species, for instance, superoxide anion radical.

### **1.3 Photocatalytic Degradation of Organic Compounds Under Light Radiation**

Several compounds such as dyes, pesticides, medicinal wastes, heavy metal cations and anions coming from industries, phenolic and organochlorine compounds are reviewed carefully for environmental remediation. Dyes are generally utilized in textile industries, and water waste of such industries after dye fixation treatment contains residues that create difficulties for treatment. Depending on functional groups, dyes can be named as azoic, anthraquinonic, heteropolyaromatic, aryl methane, xanthene, indigo, acridine, nitro, nitroso, cyanine, and stilbene.

To check catalytic activity of nano dimensional photocatalyst, generally dyes are utilized as organic substrates. As complete disposal of organic carbon content cannot be achieved by decolorization, it is not adequate by itself alone for photocatalytic degradation. Decolorization is the mineralization of dyes depending on the total organic compound (TOC) content which is important.

Catalytic degradation of photocatalyst causes the production of a radical intermediate that is followed by further conversion to provide small size different intermediates. This reaction causes the emergence of CO<sub>2</sub> of which the reaction mechanism follows the photo-Kolbe decarboxylation.<sup>19</sup>

The degradation order of dyes can be examined as follows: indigo\_phenanthrene > triphenylmethane>azo\_quinoline > xanthenes\_thiazine > anthraquinone. Besides, the conversion of heteroatoms is taking place. For example, sulfonate groups convert to sulfate ions, , primary and secondary amines to ammonium ions, azo group to nitrogen, and halogens to their related anion. Classical Langmuir–Hinshelwood kinetics is utilized to elucidate the rate of decomposition in these reactions. <sup>20</sup>

Pesticides which consist of nitrogen, phosphorous, sulfur, chlorine, and heterocyclic nitrogen atoms in their structure are widely utilized in agriculture industry. Depending on the atoms in their structure, pesticides are named as organochlorine and organophosphorous compounds. With UV light exposure, especially TiO<sub>2</sub> is widely utilized to provide degradation of basic pesticides. <sup>21,22,23</sup> Additionally, degradation of pharmaceutical compounds can be achieved via photocatalysis with TiO<sub>2</sub> under exposure of UV irradiation.

The time necessary for mineralization is greater in this case, and the formation of more stable and poisonous intermediates is observed by a majority in comparison with the parent compound. As reported, TiO<sub>2</sub> is widely used to provide mineralization of several pharmaceuticals such as antibiotics, analgesics, antipyretics, anti-inflammatory drugs, beta blockers, and anticholesteremics. <sup>24,25,26</sup>

The existence of anions and cations changes the rate of photocatalytic degradation of organic compounds. Mostly sulfate, halide, bicarbonate, nitrate, carbonate, and oxalate anions delay the degradation rate of dyes by converting the hydroxyl radicals to cause formation of corresponding anion radicals.

On the other hand, persulfate and hydrogen peroxide are oxidizing agents generating extra hydroxyl radicals during the reaction of organic compounds so that they increase the rate of degradation. Ag<sup>1+</sup>, Hg<sup>2+</sup>, Cu<sup>2+</sup>, Pb<sup>2+</sup>, Cd<sup>2+</sup>, Ni<sup>2+</sup>, and Cr<sup>6+</sup> are toxic metal ions, and for the reduction of such metal cations photocatalytically, TiO<sub>2</sub> is rather efficient.

The occurrence of metal ion reduction is achieved mainly by the production of electrons in the conduction band, and thus, dissolved  $O_2$  molecules as electron scavengers in the medium causes the delay of the rate of reduction. Besides, oxidation of organic compounds and reduction of cations at the same time is one of the emerging area of research. It was reported that metal ions increase the rate of degradation of particular organic compounds.

Several factors affect the rate of photodegradation such as pH, the amount of metal ion and organic compounds, electronic state of metal ion, and the movement of reactants and products towards active site of photocatalyst. In the UV region, undoped  $TiO_2$  with 3.2 eV band gap is satisfactory photocatalyst. Yet, the performance of the catalyst can be improved several folds when it is exposed to visible light. Therefore, this event makes the photocatalysts proper to be utilized practically in some areas in which solar radiation is used as source of light. Therefore, several system of methods have been tried until now to change the band gap of  $TiO_2$  such as doping it with several substituents such as cations or anions.<sup>27,28,29,30</sup>

Cations provide inter-band energy levels between the valence and conduction band that causes decline of band gap of doped  $TiO_2$  which is used as photocatalyst. The performance of metal ion doping to  $TiO_2$  is related with whether the energy levels of cation support the charge transfer at the interfaces or behave as recombination centers. Therefore, doping can change the rate of photocatalytic activity by increasing or decreasing.

In conclusion, no certain determination for different class of reactions can be made related with the activity of metal-doped  $TiO_2$  and undoped  $TiO_2$ . Yet, anion doping yields more successful results with  $TiO_2$  while narrowing the band gap. It provides the formation of new valence band via the mixing of anionic dopant substance and 2p orbitals of oxygen.

It is recommended that rising of valence band can be ensured via nonmetal dopant that has lower electronegativity than that of oxygen and has similar radius with oxygen to provide uniform distribution.<sup>31</sup> The other suggestion related with increased activity of anion-doped TiO<sub>2</sub> is considering the production of color centers that are actually a single or pair of electrons which is relevant with an oxygen vacancy formation.<sup>32</sup>

The photocatalytic activity of undoped TiO<sub>2</sub> in visible region can also be developed via addition of semiconductor dopants with low band gap such as CdS, PbS, CdSe, Bi<sub>2</sub>S<sub>3</sub>, with dyes as sensitizers, and cocatalysts.<sup>31</sup> This heterostructuring limits the recombination of charge carriers by separating oxidation reaction through holes and the reduction reaction through electrons at distinct sites. Under exposure of light in proportion to TiO<sub>2</sub>, CdS/TiO<sub>2</sub>, Bi<sub>2</sub>S<sub>3</sub>/TiO<sub>2</sub>, Cu<sub>2</sub>O/TiO<sub>2</sub>, and Bi<sub>2</sub>O<sub>3</sub>/TiO<sub>2</sub> heterojunction photocatalysts have demonstrated improved degradation of organic compounds.<sup>33</sup>

The achievement of improved photodegradation rate of reaction with light can additionally be done by dye-sensitized degradation which is well-known technique recently.<sup>34,35,36,37,38</sup> The important point in dye-sensitized system is that the formation of electrons in conduction band is carried out through the movement of electrons from excited state of dye, and through band gap excitation directly during UV photocatalytic reaction. Valence band holes, although they are powerful oxidizing agents, are not included in such systems, so that the performance of them in degradation reactions is supposed to be lower in UV photocatalytic reactions.

#### **1.4 ZnO as a Photocatalytic Material**

In spite of the fact that TiO<sub>2</sub> is well-known semiconducting material for photocatalysis reactions, ZnO also seems to be proper choice due to its desired optoelectronic, catalytic and photochemical properties together with its low cost. ZnO has band gap with 3.0 eV value narrower compared to anatase form of TiO<sub>2</sub>. The position of valence band of ZnO provides the formation of photogenerated holes with powerful oxidizing ability to degrade several organic compounds.<sup>39</sup>

Until now, degradation ability of ZnO has been checked with solutions of different dyes,<sup>40,41,42,43,44</sup> and several other contaminants that pollute environment.<sup>45,46,47,48</sup> In several cases, ZnO has been submitted as more effective compared to TiO<sub>2</sub>,<sup>45,46,49,50</sup> yet the case of photocorrosion<sup>51</sup> and sensitivity of ZnO towards easy dissolution at high pH limit the application of it importantly as photocatalyst.

Kislov et al.<sup>52</sup> demonstrated that crystallographic orientation extremely affects the photoactivity and photostability of ZnO materials that has single crystal structure.

Many studies have reported that under exposure of visible irradiation, ZnO was reasonably operative to provide decomposition of several organic compounds in aquatic environment.<sup>43,53</sup> For example, the decolorization and decomposition of methyl green was achieved via ZnO under exposure of visible light with low energy power, and besides when an oxidizing agent such as Na<sub>2</sub>S<sub>2</sub>O<sub>8</sub> and H<sub>2</sub>O<sub>2</sub> were added, the decomposition rate of pollutant improved. ZnO was utilized by Lu et al.<sup>43</sup> under visible light for degradation of Basic Blue 11, and the studies were done to understand the effects of potential factors such as preliminary dye concentration, amount of catalyst, and preliminary pH. According to Pare et al.,<sup>53</sup> the photocatalytic degradation of acridine orange can be enhanced by adding proper amount of hydrogen peroxide and potassium persulphate, whereas the activity greatly can be decreased by adding inert salts such as NaCl and Na<sub>2</sub>CO<sub>3</sub>.

On the other hand, Sakthivel et al.<sup>54</sup> investigated the activity of both ZnO and TiO<sub>2</sub> by solar radiation degradation of Acid Brown 14 which is one of the organic pollutants. According to the results of photodegradation rate experiments, the superior rate value was obtained for ZnO that exhibits absorption of great number of solar spectrum and absorption of large amount of light irradiation compared to TiO<sub>2</sub>. Dindar and İçli<sup>55</sup> reported that under exposure of sodium lamp and direct sunlight, the degradation of phenol was taking place more effectively for TiO<sub>2</sub>. Yet for ZnO, intensive sunlight is necessary to be reactive as TiO<sub>2</sub>. This result is not found as logical and not extraordinary, because distinct catalysts have tendency to exhibit similar activity under exposure of concentrated sunlight, because after this time the rate determining factor is not the production of photoactive species, on the contrary, mass transfer restriction of pollutant to the surface of photocatalyst.

According to Pardeshi and Patil,<sup>56</sup> photodegradation of phenol was achieved more efficiently under exposure of solar light compared to artificial visible light. Additionally, although ZnO was reused for five times, it faced with photocorrosion exclusively in small proportions. In conclusion, under exposure of sunlight, ZnO is more appropriate compared to TiO<sub>2</sub> for catalytic photodegradation.

The catalytic efficiency of ZnO via solar assisted photodegradation of Direct Blue 53 was enhanced by addition of activated carbon with distinct amounts in aquatic medium to ZnO by Sobana and Swaminathan.<sup>57</sup> After this mixing, the synergistic effect raised the performance of the catalyst by a factor of 4.21. According to Comparelli et al.,<sup>58</sup> the existences of deactivating molecules that find on the surface of ZnO protect the photocatalyst from photocorrosion and dissolution at distinct pH values. As mentioned in literature, hybridization of ZnO at the surface with carbon layers similar to graphite stopped photo-oxidation of ZnO nanomaterials and increased the photocatalytic performance of ZnO.<sup>59</sup> Prevention of photo-oxidation and improvement in the performance of photocatalyst were also acquired when the hybridization of ZnO with polyaniline monolayer was achieved.<sup>60</sup>

ZnO until now has seldom been checked as photocatalyst in gas solid samples in spite of being more effective compared to commercial and home prepared TiO<sub>2</sub> related with photodegradation of ethanoic acid.<sup>61</sup> Hexagonal ZnO nanoparticles with high surface area indicated better photodegradation of gaseous (CH<sub>3</sub>)<sub>2</sub>S<sub>2</sub> that is a rigid pollutant when ZnO powder was utilized.<sup>62</sup>

The synthesis of ZnO nanomaterials was made by El-Kemary et al.<sup>63</sup> by mixing zinc acetate compound with triethylamine in ethanol at the temperature of 50–60 °C for 1 hour. The photocatalytic performance of the catalyst for photodegradation of ciprofloxacin was determined with UV light exposure. The degradation rate was efficient at pH 7 and 10 values, but the rate decreased at pH 4.

When ZnO nanomaterials synthesized from zinc acetate by triethylamine template provided sol-gel precipitation and additional hydrothermal treatment increased the proportion of conversion for oxidation of phenol by light. Additionally, via further calcinations treatment, higher conversion values were acquired compared to experiments when Degussa P25 was utilized. In another research, ZnO nanoparticles were synthesized by utilizing zinc acetate and precipitated with NaOH, and these nanoparticles were used to achieve photodegradation of Biebrich scarlet in aquatic medium.<sup>44</sup>

The experiments which were made with commercial semiconductors such as TiO<sub>2</sub>, ZnO, CdS and ZnS exhibited that ZnO nanoparticles was the most active photocatalyst for dye decolorization, because, at basic medium (nearly at pH 10), the low dissociation of ZnO was recognized and its performance changed a little after three cycles.

ZnO nanoparticles can also be synthesized via thermal decomposition technique by using zinc oxalate in the absence of any additional materials and solvents, and it was determined that ZnO nanostructures are more effective compared to commercial ZnO during the mineralization process of Reactive Red 120 under exposure of solar irradiation.<sup>64</sup> Polydispersed ZnO nanoparticles with distinct particle sizes (nearly 120 and 30 nm) were synthesized by Kitture et al.<sup>65</sup> to control photodegradation of MB and MO organic dyes under exposure of sunlight. According to their results, large nanoparticles were more stable against photocorrosion and the activity of larger sized particles were higher compared to smaller sized ZnO nanoparticles and P25. Additionally, uniform ZnO nanorods with proper arrangement were prepared via microwave-assisted chemical deposition technique onto the surface of indium tin oxide substrates.<sup>66</sup>

For the photodegradation of MB under UV light, nanorod structures were effective and their performance showed size-dependency. Hierarchically structured porous ZnO spherical nanostructures exhibited better degradation activity for phenol compared to nanoparticles of TiO<sub>2</sub>.<sup>67</sup> According to Li et al.,<sup>68</sup> ZnO hollow spheres showed enhanced photoreactivity by a factor of 4.66 for photodecomposition of unstable brilliant red X-3B when compared with ZnO nanostructures.

Additionally, Mohajerani et al.<sup>69</sup> prepared ZnO nanoparticles with distinct shapes such as rods, flower-like, and microsphere to check the effect of shape particles for photodegradation of CI acid red 27 under exposure of direct sunlight. The nanorods showed a little bit better photocatalytic activity than nanoparticles. On the other hand, flower-like and microsphere 3D nanostructures had inferior photoactivity.

In literature, it was mentioned that ZnO nanoflowers had superior photoactivity compared to ZnO nanorods during degradation of 4-chlorophenol with UV light.<sup>70</sup> The better activity of nanoflower structure is related with high amount of oxygen vacancy at the surface of 1D nanostructure. Besides, flower like 3D hierarchically structured microstructures that was synthesized with low temperature in aquatic medium were more effective compared to distinct nanostructures such as nanoparticles, nanosheets, and nanorods of ZnO.<sup>71</sup>

Photocatalytic performance can be enhanced via hybrid nanostructures that consist of semiconducting material-metal nanoparticles and semiconducting material- graphene nanocomposite combinations. According to some reports, with the addition of noble metal nanoparticles such as Au, Ag, Pt and graphene to hybrid ZnO and TiO<sub>2</sub> nanostructures, the photocatalytic activity can be increased.<sup>72,73,74</sup> In such distinct structured systems, noble metal particles behave as electron scavenging centers to provide formation of electron and hole pairs efficiently that result in the raise of performance of photocatalyst.<sup>75,76</sup>

## **1.5 Conjugated Polymers for Photocatalysis**

For last twenty years, conjugated polymers have gained great importance because of distinct application areas. The successful application of such polymers can be mentioned as organic electronic devices such as light emitting diodes, field effect transistors, and solar cells.<sup>77</sup> For the studies related with the enhanced performance of a photocatalyst, semiconductor nanoparticle recently were embedded into the conjugated polymers.<sup>78</sup> Ppy (polypyrrole) films that consist of TiO<sub>2</sub> were used as catalyst to degrade the methylene blue and methyl orange dyes with UV light irradiation. The Ppy/TiO<sub>2</sub> composite films had superior degradation reaction rate when the suspension of TiO<sub>2</sub> nanoparticle was utilized exclusively.

When TiO<sub>2</sub> in polyethylene8 and poly(vinyl chloride) (PVC)<sup>79</sup> composites consist of nonconducting polymers, the degradation of these polymers is observed with UV light. Yet, there is no such a degradation with conjugated polymers is observed in the availability of TiO<sub>2</sub> with UV light irradiation. The usage of semiconducting materials can be classified as environmental remediation consist of degradation of several distinct compounds such as alkanes, aliphatic alcohols, carboxylic acids, alcohols, phenols, aromatic carboxylic acids, dyes, simple aromatics, halogenated alkanes and alkenes, surfactants, and pesticides, at the same time, as the deposition of heavy metals such as Pt<sup>4+</sup>, Au<sup>3+</sup>, Rh<sup>3+</sup>, and Cr<sup>6+</sup> by reduction from an aquatic medium to surfaces.<sup>80,81,82</sup>

In several reports, total mineralization of organic pollutants have been announced. Within the popular photocatalysts, especially anatase form of TiO<sub>2</sub> has been widely utilized in different studies because of its stability and versatility.<sup>83</sup> Besides, for activation of TiO<sub>2</sub>, UV light irradiation is necessary due to its huge band gap value with 3.2 eV. In theory, a conjugated polymer that has the same band gap with a semiconductor can be used as photocatalyst. Yet, in reality, selection of conducting polymers as photocatalyst can be done by adjusting its band gap via enhancing absorption and conversion capacity to solar spectrum. To obtain a proper photocatalyst, stable and eco-friendly conducting polymers with appropriate semiconductor band gap should be prepared.

For the selection of conjugated polymers, especially poly (3,4-ethylenedioxythiophene) (PEDOT) offers several advantages such as being polymerized regioregularly, and stable, having narrow band gap, optical transparent properties.<sup>84,85,86</sup> Recently, for distinct application areas, conjugated polymers are synthesized as including metal nanoparticles. Such polymers are utilized as support while embedding metal nanoparticles and the obtained materials exhibit high photocatalytic activity.<sup>87,88</sup>

## 1.6 Separation Process of Photocatalysis

For water treatment, distinct semiconductors have been reported as proper photocatalyst, yet, practically, effective separation and recycling of these small sized photocatalyst powders are still problematic.<sup>89,90</sup> Besides, when the size of photocatalyst is reduced to nano-size, this reduction of size again causes difficulty in separation. Therefore, for collecting particles of semiconductor photocatalyst, finding easy and efficient procedure is really satisfactory. Having magnetic property of photocatalyst for separation can solve the problem of this issue.<sup>91</sup>

Immobilization of magnetic particles to produce hybrid materials provides collection of photocatalyst particles via magnet, acquisition of perfect surface chemistry property, superior mechanical properties, and proper thermal stability. Besides, there is another difficulty with dispersion of photocatalyst in aqueous medium that affects activity of it undesirably. As a result, low dispersion results in the low interaction between photocatalyst and molecules of organic pollutant.<sup>92</sup> Recently, as reported in several research, low dispersion of photocatalyst in aqueous medium that decreases the performance of the catalyst has been trying to be eliminated via supported materials in nano-size that consist of magnetic nanoparticles.

## 1.7 Aim of the Study

In this study, nanocomposite material in which  $\text{SiO}_2\text{-CoFe}_2\text{O}_4$  and ZnO supported on PEDOT polymer, ( $\text{SiO}_2\text{-CoFe}_2\text{O}_4\text{/PEDOT/ZnO}$ ) was prepared by using a facile method. After that the characterization of the prepared catalyst and their components were performed by using VSM, SEM, TEM and HR-TEM. Finally the photocatalytic activity of the prepared catalyst was measured in the removal of methylene blue (MB) which is known as stimulant of textile wastewater under UV light exposure at room temperature.

## CHAPTER 2

### MATERIALS AND METHODS

#### 2.1. Materials

Cobalt (II) chloride hexa-hydrate ( $\text{CoCl}_2 \cdot 6\text{H}_2\text{O}$ ), iron(III) chloride hexa-hydrate ( $\text{FeCl}_3 \cdot 6\text{H}_2\text{O}$ ), (3-Aminopropyl)trimethoxysilane (APTMS), tetraethylorthosilicate (TEOS), ammonium hydroxide ( $\text{NH}_4\text{OH}$ ), 3,4 ethelenedioxythiophene (EDOT), zinc oxide (ZnO) nanoparticles, chloroform ( $\text{CHCl}_3$ ), and methylene blue (MB) were purchased from Sigma-Aldrich as analytical grade and used directly. In all study deionized water produced by Milli-Q Water Purification System was used.

#### 2.2. Characterization and Instrumentation

Field Emission Scanning Electron Microscopy (FE-SEM) was used to characterize size and shape of nanoparticles. The model of instrument is Quanta 400 FE-SEM from FEI. The suspension solutions of samples were dropped onto the grids coated with carbon tape after that, the samples were left overnight for drying and then analyzed.

The JEOL JEM-2010F transmission Electron Microscopy (TEM) and high resolution-TEM (HR-TEM) was used to characterize size and shape of nanoparticles. The instrument is an advanced field emission electron microscope with an accelerating voltage of maximum 200 kV.

Energy-dispersive X-ray analyzer (EDX) coupled with SEM and TEM were used to indicate elemental composition of the prepared samples.

Labor-UV-reactor-System 2 (UV-RS-2) was utilized for photocatalytic applications and Specord S 600 UV-Vis spectrometer was applied for following the degradation of dye (MB).

### **2.3. Preparation of Silica Coated Cobalt Ferrite (SiO<sub>2</sub>-CoFe<sub>2</sub>O<sub>4</sub>) Magnetic Nanoparticles**

Firstly, cobalt ferrite (CoFe<sub>2</sub>O<sub>4</sub>) magnetic nanoparticles were synthesized as magnetic core part via co-precipitation method.<sup>93</sup> The preparation procedure can be seen in Figure 2.1. For the synthesis of magnetic nanoparticles, 25 mL of 0.4 M FeCl<sub>3</sub>.6H<sub>2</sub>O and 25 mL 0.2 M CoCl<sub>2</sub>.6H<sub>2</sub>O solutions were prepared and mixed, and 25 mL of 3.0 M NaOH and 12.5 mL of 1.5 M NaCl solutions were added to this mixture drop by drop slowly and left mixing for an hour at 80 °C in ultrasonic bath. After 1 hour passes, the external magnet was utilized to collect precipitated nanoparticles and rinsed with deionized water. The preparation procedure is given in Figure 2.1.

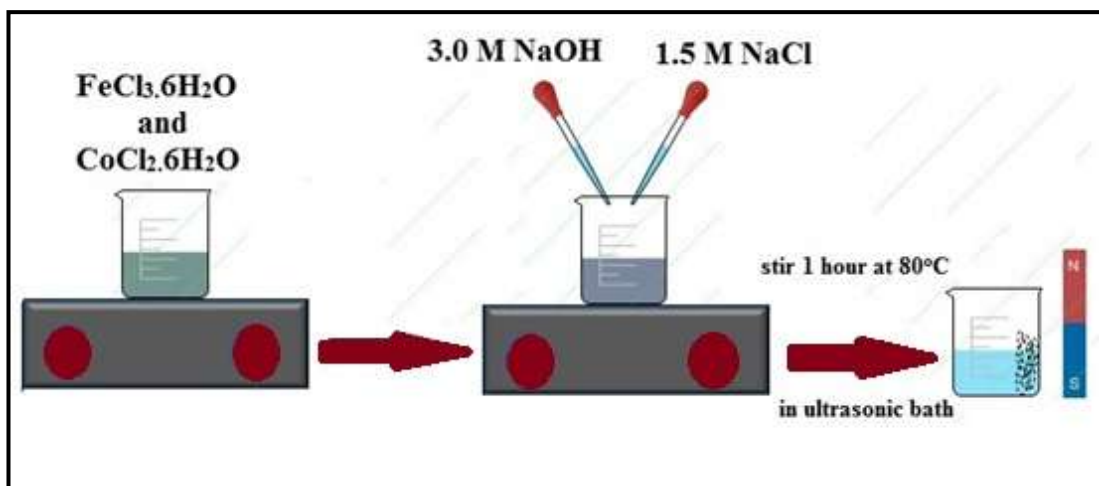


**Figure 2.1** The preparation procedure of  $\text{CoFe}_2\text{O}_4$  magnetic nanoparticles.

The addition of silica shell to core magnetic nanoparticles was achieved via Stöber method.<sup>94</sup> The procedure of silica shell to nanoparticles can be seen in Figure 2.2. For silica coating,  $169 \mu\text{L}$  TEOS and  $14.4 \mu\text{L}$  APTMS were added to the ethanol solution, later on  $20 \text{ mL}$   $\text{CoFe}_2\text{O}_4$  magnetic nanoparticle solution was added to this mixture and left for stirring at room temperature for 3 hours. After this time, again external magnet was used for collecting and prepared particles were washed via water-ethanol mixture.

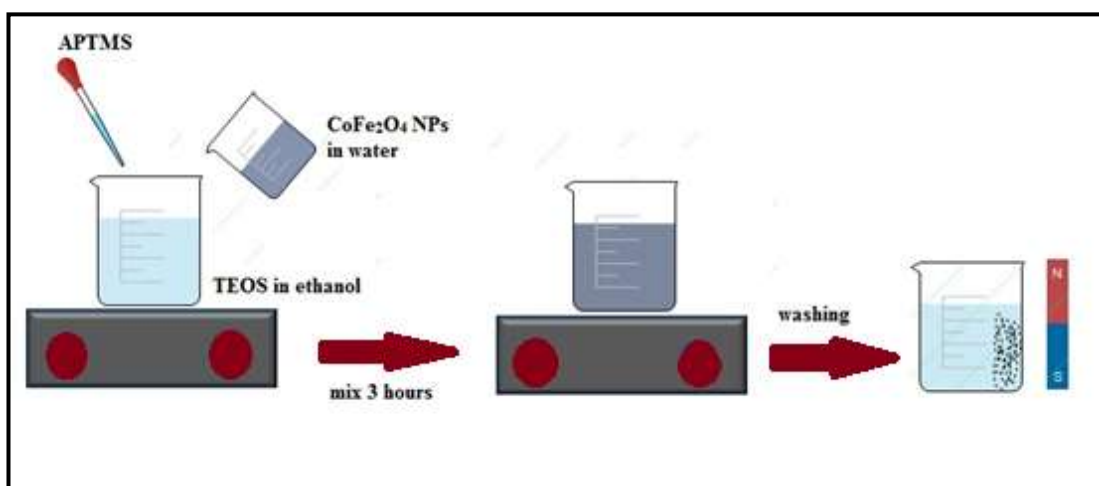


**Figure 2.2** Silica coating over  $\text{CoFe}_2\text{O}_4$  nanoparticles.

## 2.4. Preparation of PEDOT

For the synthesis of Poly (3, 4 ethelenedioxythiophene) (PEDOT), chemical polymerization of EDOT was done. This procedure contains addition of solution of 0.550 g iron (III) chloride ( $\text{FeCl}_3$ ) in 5 ml  $\text{CHCl}_3$  to 0.284 g EDOT in 5 ml  $\text{CHCl}_3$  dropwise on magnetic stirrer. Then, the mixture was left mixing for 3 hours at room temperature to complete polymerization. After 3 hours reaction time, 30 mL methanol was added to this mixture and put into the refrigerator for 1 day for precipitation. Later on, the precipitates of PEDOT was collected via filtration and washed with methanol by using Soxhlet extraction apparatus for 2 days. Later on, the synthesized PEDOT was left for drying at room temperature. The preparation procedure is given in Figure 2.3.

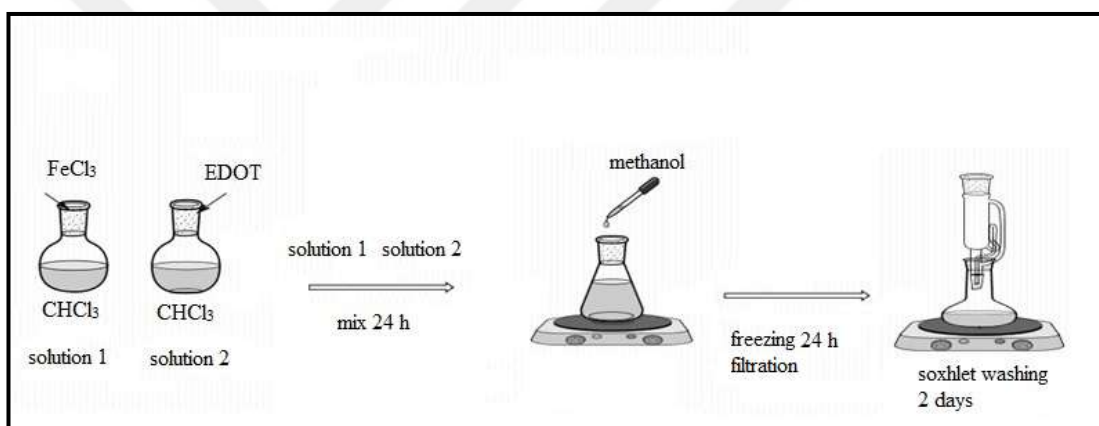


**Figure 2.3** Preparation of PEDOT

## 2.5. Preparation of PEDOT/ZnO and $\text{SiO}_2\text{-CoFe}_2\text{O}_4\text{/PEDOT/ZnO}$ Nanocomposite Material

PEDOT/ZnO and  $\text{SiO}_2\text{-CoFe}_2\text{O}_4\text{/PEDOT/ZnO}$  nanocomposite material was prepared by chemical polymerization of EDOT method. For the first structure only ZnO nanoparticles were used. For the magnetic nanocomposite ZnO nanoparticles and  $\text{SiO}_2\text{-CoFe}_2\text{O}_4$  magnetic nanoparticles were used to prepare it.

For synthesis, firstly, 0.350 g Iron (III) chloride ( $\text{FeCl}_3$ ) was dissolved in 5 ml of  $\text{CHCl}_3$ , later on 0.04 g ZnO nanoparticles were added on magnetic stirrer and waited for 5 min for mixing. In another beaker, 0.175g EDOT was added to 5 ml  $\text{CHCl}_3$  and mixed well on magnetic stirrer for 5 min. Later on, preliminary solution was added to the second solution dropwise. At the end, 0.10 g silica coated  $\text{CoFe}_2\text{O}_4$  magnetic nanoparticles were added to this mixture and left stirring for extra 24 hours to complete polymerization at room temperature. After 24 hours mixing, 25 ml ethanol was added to the prepared mixture and put into refrigerator for precipitation for 1 day.

After precipitation process, the synthesized precipitates of  $\text{SiO}_2\text{-CoFe}_2\text{O}_4\text{/PEDOT/ZnO}$  were collected via external magnet and rinsed with methanol for 3 days with Soxhlet extraction apparatus. Later on, the prepared nanocomposite was dried. The same procedure was followed for preparation of PEDOT/ZnO and  $\text{SiO}_2\text{-CoFe}_2\text{O}_4\text{/PEDOT}$  nanostructures. The preparation procedure is given in Figure 2.4.

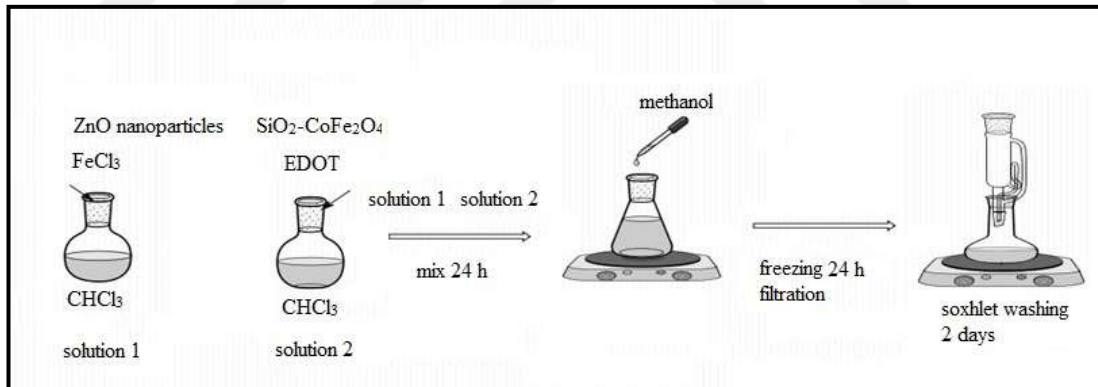


**Figure 2.4** Preparation of  $\text{SiO}_2\text{-CoFe}_2\text{O}_4\text{/PEDOT/ZnO}$  nanocomposites.

## 2.6. Determination of Catalytic Performance of the Prepared Materials

For photocatalytic activity, to achieve adsorption-desorption equilibrium, firstly 0.01 g of photocatalyst was added to 10 mL methylene blue (MB) dye solution and mixed in the dark. After obtaining constant concentration of MB, the mixture was exposed to UV radiation via lamp with the power of 300 W on magnetic stirrer, and uniform mixing of photocatalyst with dye solution was achieved (Figure 2.5).



**Figure 2.5** Photocatalytic reactor used in this study

For decolorisation tests of dye, 2 mL sample was taken from the reactor via a syringe, and controlled at every 10 min intervals. The maximum absorbance value of remaining portion of dye at 660 nm was followed via UV-Vis spectrophotometer given in Figure 2.6. The photocatalytic degradation rate of dye was calculated via using absorbance value (A) that was acquired according to Eq. 1.

$$D = (A_0 - A_t) / A_0 \times 100 \% \quad (1)$$

( $A_0$ =initial absorbance of MB,  $t$ = reaction time,  $A_t$ =absorbance at time t)



**Figure 2.6** UV-Vis spectrophotometer used for decolorisation experiments.

## CHAPTER 3

### RESULTS AND DISCUSSION

Increment in the environmental pollution is one of the greatest issues that the world is facing today. Developed and developing countries are trying to prevent the effects of this huge problem. Anthropogenic sources based air, soil and water pollution causes the instability of the ecosystem and these sources require continuous remediation. Every day, several pollutants such as sulfur oxides (SO<sub>x</sub>), nitrogen oxides (NO<sub>x</sub>), volatile organic compounds (VOCs), carbon monoxide (CO), ammonia (NH<sub>3</sub>), and harmful chemicals like benzene, polycyclic aromatic hydrocarbons (PAHs), heavy metals, chlorinated organic compounds, dyes, detergents, surfactants, and harmful agricultural wastes are being released to the environment randomly. Thanks to science and technology, the pollution issue can be solved and the environment will be renovated. This can be achieved via a photocatalyst.

The term photocatalyst is formed with the combination of “photo” and “catalyst”. Catalyst is a substance that is used to decrease activation energy so that it results in the increment of reaction rate without being any change and expended. As a broad meaning, in photocatalytic reactions, radiation is utilized to provide activation of a substance which alters the rate of reaction without being involved. Therefore, the function of photocatalyst is to change the rate of the reaction by using light.

Via light irradiation, the photocatalyst can form very reactive molecules called as free radicals from water and oxygen coming from air. These radicals can enable to convert substances to comparatively harmless chemicals by breaking the structure of them.

A photocatalyst can be greatly utilized for purification of water and air, self cleaning, and self-sterilizing surfaces and antifogging surfaces. On the other hand, a photocatalyst can also be used for dealing with anticorrosive surfaces, lithography, photochromic materials, microchemical systems, for the synthesis of organic compounds selectively and eco-friendly, and for the production of hydrogen. Recently, one of the most effective applications of heterogeneous photocatalyst is to decrease environmental pollution. For this, semiconductor-based photocatalysts are good candidates for the complete removal of polluting organic compounds that present air and wastewater sources. The photocatalytic system of a heterogeneous catalyst consists of photoinduced transformations of molecules and reactions at catalyst surface.

In this study, to produce a material with high photocatalytic activity and magnetic separation property, a facile polymerization method was demonstrated to fabricate a magnetically recyclable novel PEDOT modified ZnO ( $\text{SiO}_2\text{-CoFe}_2\text{O}_4\text{/PEDOT/ZnO}$ ) photocatalyst material. The detailed characterization and catalytic activity investigation were performed for the produced materials.

### **3.1. Preparation and Characterization of Magnetic Cobalt Ferrite Nanoparticles with Silica Shell**

For the synthesis of cobalt ferrite ( $\text{CoFe}_2\text{O}_4$ ) magnetic nanoparticles, modified co-precipitation procedure was applied. By using this procedure, extremely dispersed small magnetic nanoparticles and the agglomerates were produced.

The formed magnetic nanoparticles, later on, were coated by silica shell to decrease the interaction among the nanoparticles which cause in the formation of larger particles. The silica coverage is also proper for the attachment of metal ions to the surface of catalyst. For silica coating, Stöber method was selected to coat magnetic core as mentioned in experimental part in detail.

TEM was utilized to exhibit the morphological properties of magnetic-silica core-shell structure. The synthesized silica coated cobalt ferrite nanoparticles were figured out (Figure 3.1). As seen from the Figure 3.1, the silica coated magnetic nanoparticles have size with average diameter of 14-20 nm and the aggregates with nearly 150 nm.

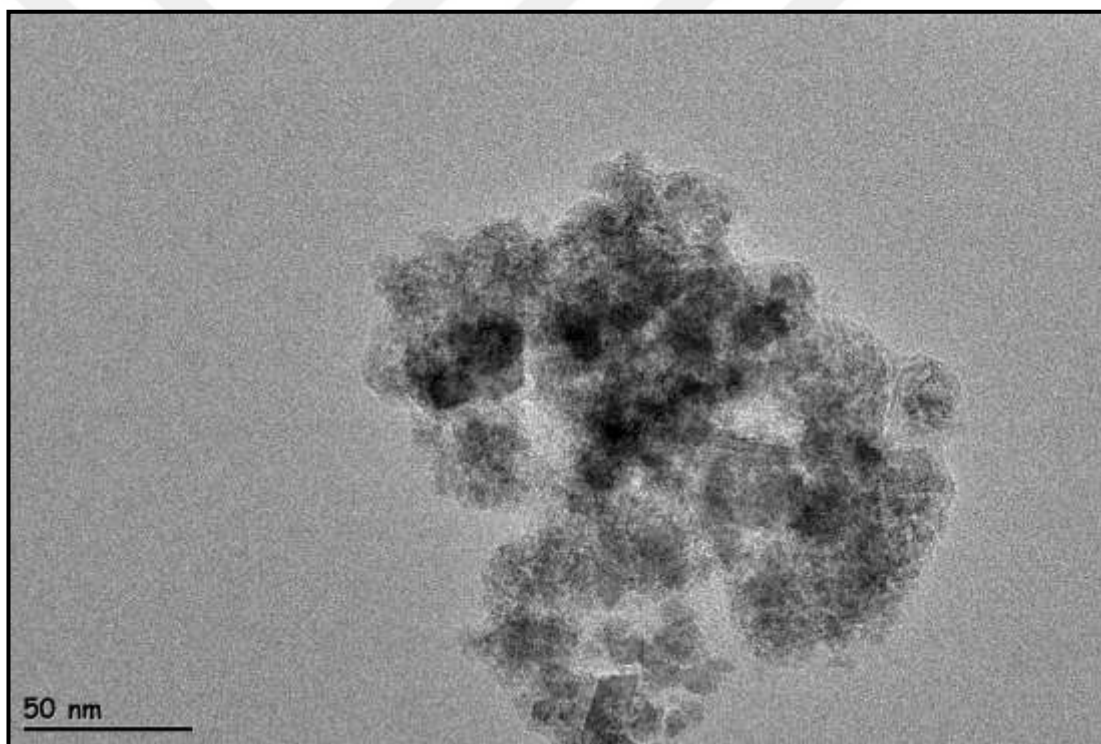


**Figure 3.1** TEM image of the prepared  $\text{SiO}_2\text{-CoFe}_2\text{O}_4$  magnetic nanoparticles.

Silica shell around the magnetic nanoparticles was examined via the analysis of energy dispersive X-ray (EDX). EDX results of silica coated cobalt ferrite magnetic nanoparticle exhibit the existence of silica in the structure. Copper signal is resulting from the sample grid.

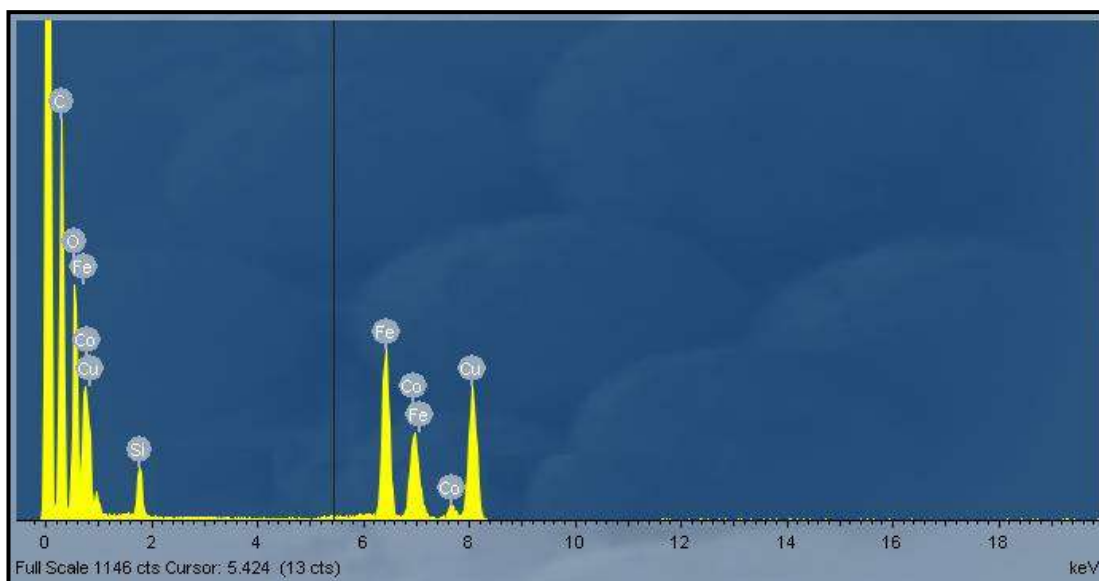
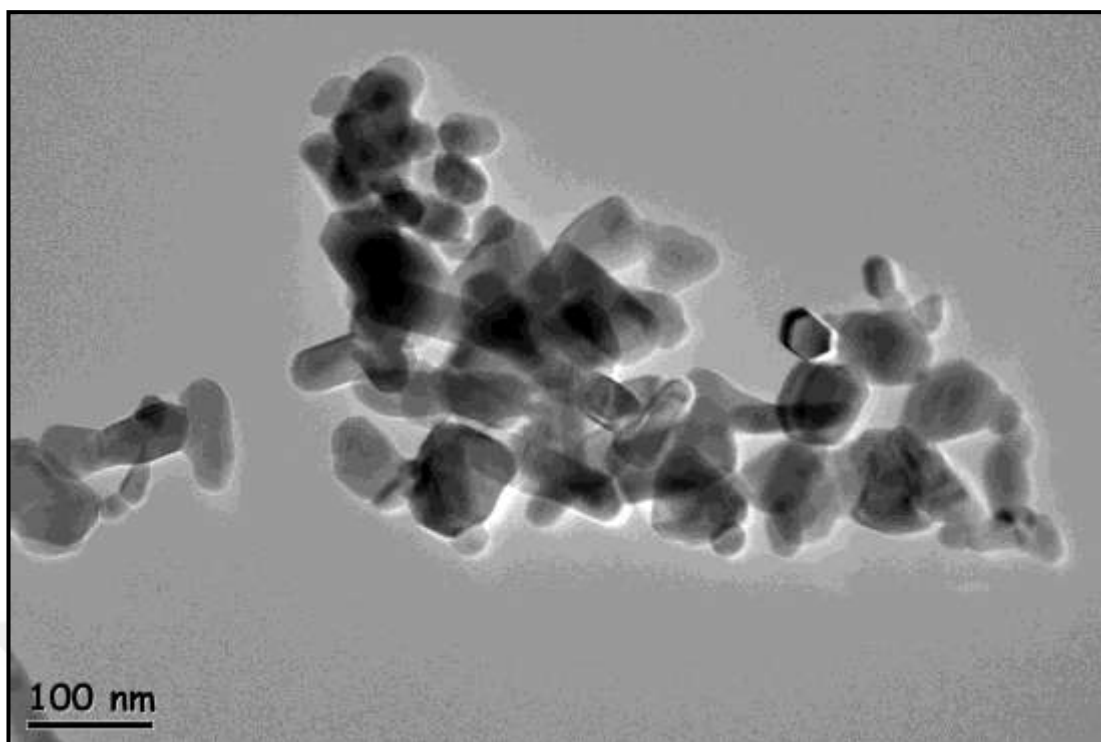


**Figure 3.2** EDX patterns of  $\text{SiO}_2\text{-CoFe}_2\text{O}_4$  magnetic nanoparticles.

### **3.2. Preparation and Characterization of Nanomaterials Prepared in This Study**

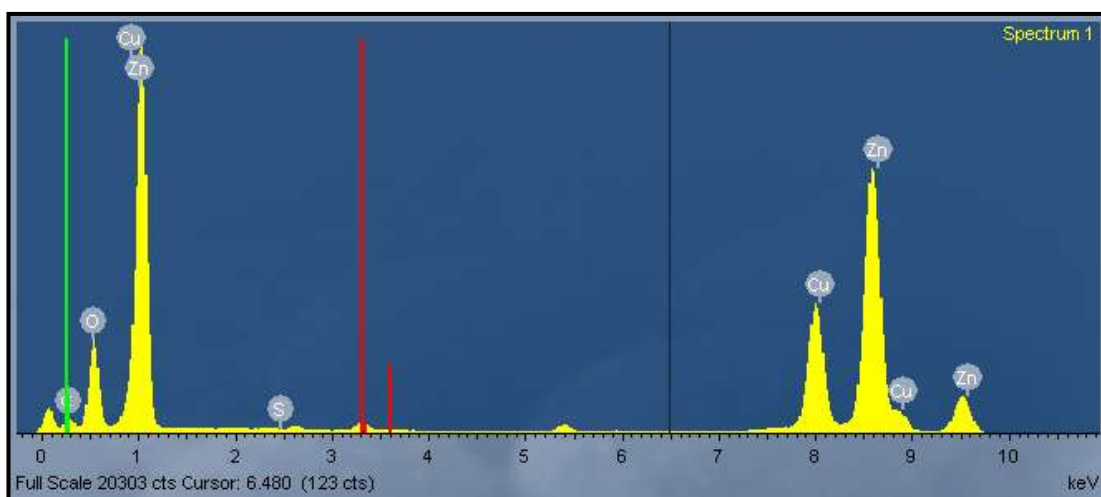
Scanning electron microscopy (SEM), transmission electron microscopy and energy dispersive X-ray spectroscopy (EDX) coupled with SEM and TEM were utilized to make the structure and morphological analysis of ZnO nanoparticles, PEDOT and  $\text{SiO}_2\text{-CoFe}_2\text{O}_4\text{/PEDOT/ZnO}$  nanocomposite material.

Figure 3.3-3.5 exhibits the morphological analysis of ZnO nanoparticles, PEDOT and  $\text{SiO}_2\text{-CoFe}_2\text{O}_4\text{/PEDOT/ZnO}$  nanocomposite materials, respectively. According to TEM image given in Figure 3.3, the particle size of the ZnO ranges from 50 nm to 100 nm.



**Figure 3.3** TEM image of ZnO nanoparticles.

After getting TEM image, EDX measurement of ZnO nanoparticles also performed. An obtained result is given in Figure 3.4.



**Figure 3.4** EDX pattern of ZnO nanoparticles.

The morphological property of PEDOT was investigated with SEM measurements and obtained image is given in Figure 3.5.

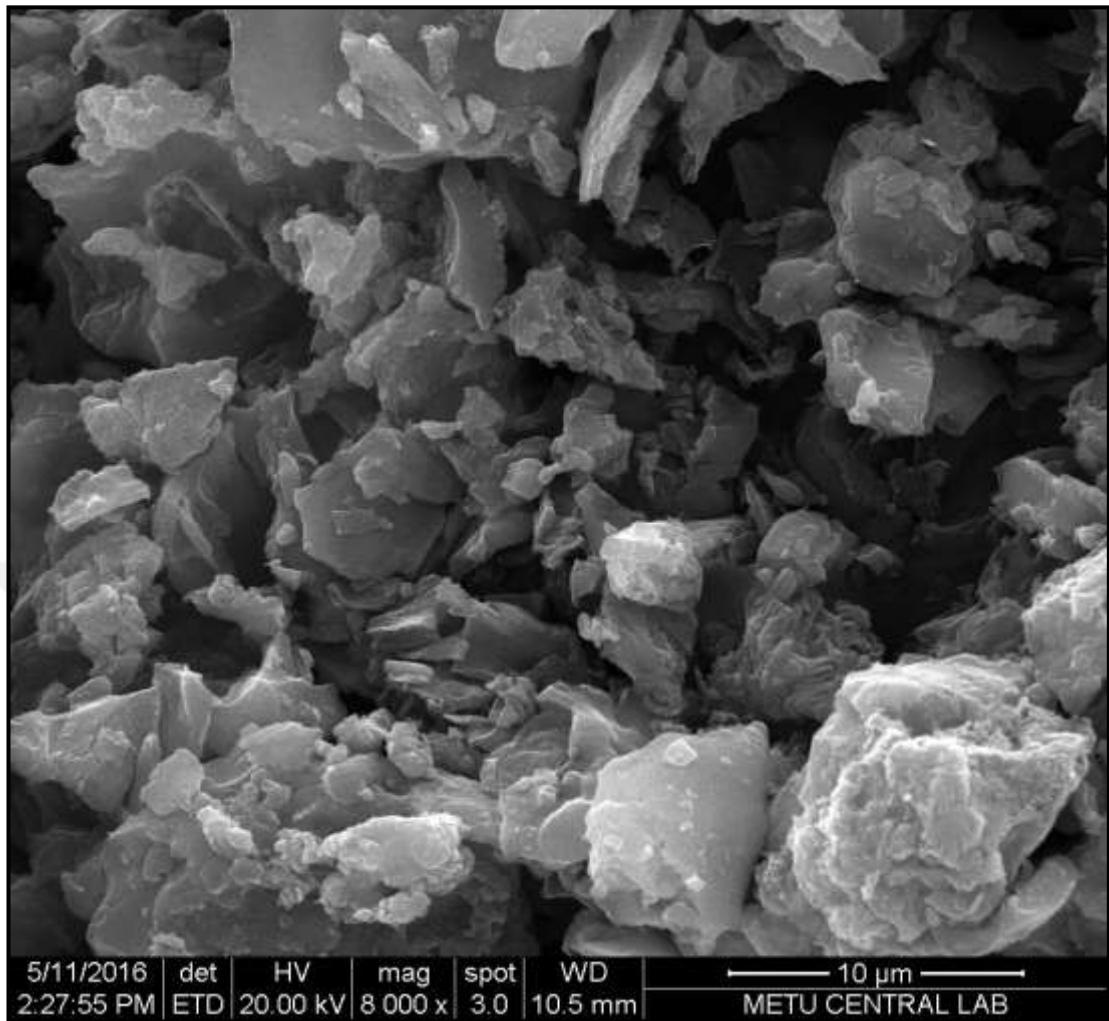


**Figure 3.5** SEM image of PEDOT.

Finally TEM image of  $\text{SiO}_2\text{-CoFe}_2\text{O}_4\text{/PEDOT/ZnO}$  nanocomposite material was obtained. Obtained result is given in Figure 3.6.

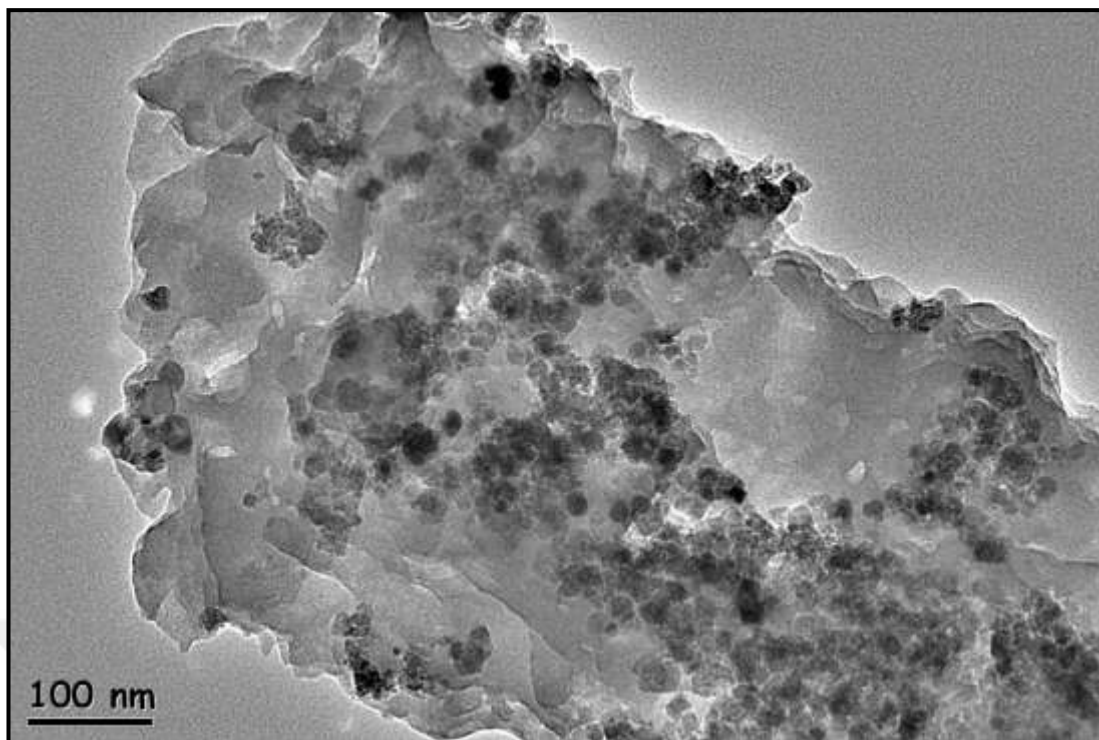


**Figure 3.6** TEM image of  $\text{SiO}_2\text{-CoFe}_2\text{O}_4/\text{PEDOT}/\text{ZnO}$  nanocomposite material.

As can be seen from Figure 3.6, silica coated magnetic nanoparticles and ZnO nanoparticles placed into PEDOT polymer, which holds the whole structure together.

Elemental composition of prepared nanocomposite material was examined via EDX coupled with SEM. According to EDX pattern of prepared  $\text{SiO}_2\text{-CoFe}_2\text{O}_4/\text{PEDOT}/\text{ZnO}$  nanocomposite material, the final structure consists of all elemental frames of  $\text{SiO}_2\text{-CoFe}_2\text{O}_4/\text{PEDOT}/\text{ZnO}$  (Si, O, Co, Fe, and Zn).

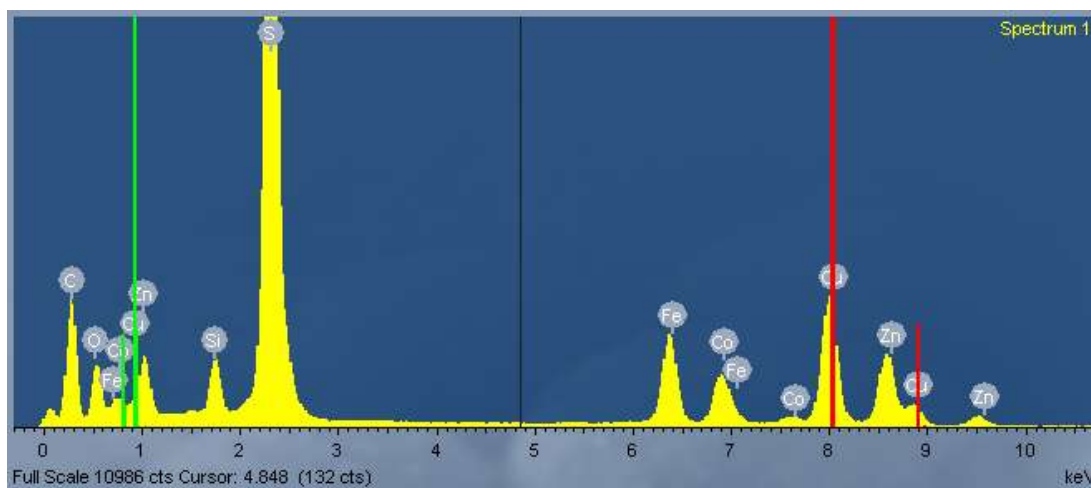


**Figure 3.7** EDX patterns of SiO<sub>2</sub>-CoFe<sub>2</sub>O<sub>4</sub>/PEDOT/ZnO nanocomposite material.

### 3.3. Magnetic Property of Prepared SiO<sub>2</sub>-CoFe<sub>2</sub>O<sub>4</sub>/PEDOT/ZnO Nanocomposite Material

External magnet was utilized to check magnetic behavior of SiO<sub>2</sub>-CoFe<sub>2</sub>O<sub>4</sub>/PEDOT/ZnO nanocomposite. For this, the synthesized nanocomposite was put near external magnet and collection time was measured (Figure 3.8). 30 seconds is enough for nanocomposite material to be collected totally by magnet.



**Figure 3.8** Magnetic behavior of SiO<sub>2</sub>-CoFe<sub>2</sub>O<sub>4</sub>/PEDOT/ZnO nanocomposite material under external magnetic field (1.6 T).

### 3.4. Photocatalytic Activity Studies of the Prepared Materials

The photocatalytic activity test of SiO<sub>2</sub>-CoFe<sub>2</sub>O<sub>4</sub>/PEDOT/ZnO nanocomposite materials and other components were done via degradation of organic azo-dye called as methylene blue (MB) which is well known pollutant in textile industry. It was probe reaction which was measured with the exposure of UV light irradiation.

MB is highly toxic and has complex structure, for this reason, the physical and biological techniques are insufficient for the treatment of this dye. Therefore, MB was chosen as simulant of textile wastewater. The comparison of prepared nanocomposite was done with ZnO nanoparticles, PEDOT polymer and ZnO/PEDOT composite material.

Aqueous suspension of 10 mL MB with 1 A was put in a reactor and 0.01 gram of prepared photocatalysts were added. Before exposure of MB and catalyst mixture with UV light, to provide adsorption-desorption equilibrium, the mixture was mixed in the dark on magnetic stirrer. During UV light exposure, stirring continued to prevent adhering of the photocatalyst. The reaction was taking place at room temperature via water cooling. In each 10 min intervals, 2 mL sample solution was taken, and to extract catalyst particles exactly, centrifuge and external magnet was utilized. UV-Vis spectrophotometer was used to measure absorbance value of MB at 660 nm. The degradation rate (D) of MB was followed by using absorbance values of it depending on equation 1 in Experimental part. The same conditions are continued during the all studies.

In addition, control experiments were done by exposing MB solution to UV-light radiation with absence of catalyst under same experimental conditions before starting to basic experiments. Without catalyst, no difference in absorbance value of MB solution was observed.

### **3.4.1. Adsorption-Desorption Profiles of the Prepared Nanostructures**

Finding the adsorption/desorption behavior of the prepared catalyst is an important step in the degradation of pollutants with photocatalytic process. For this reason, before starting to UV light irradiation, the MB solution and photocatalyst mixture was stirred magnetically in the dark to figure out the adsorption/desorption equilibrium. For this 10 mg of photocatalyst was mixed with MB under dark for different durations and the absorption maxima of MB located at about 660 nm was followed. The adsorption/desorption equilibrium was reached after 10 min and maximum 10 % decrease were recorded for the SiO<sub>2</sub>-CoFe<sub>2</sub>O<sub>4</sub>/PEDOT/ZnO nanocomposite materials.

### **3.4.2. Photocatalytic Activity of the Prepared Nanostructures**

ZnO nanoparticles, PEDOT polymer and ZnO/ PEDOT composite material were chosen as the reference photocatalysts for comparison with the SiO<sub>2</sub>-CoFe<sub>2</sub>O<sub>4</sub>/PEDOT/ZnO nanocomposite materials. Photocatalytic decolorization of methylene blue under UV light illumination was started with ZnO nanoparticles. Obtained results in the presence of 10 mg ZnO nanoparticles are given in Figure 3.9.

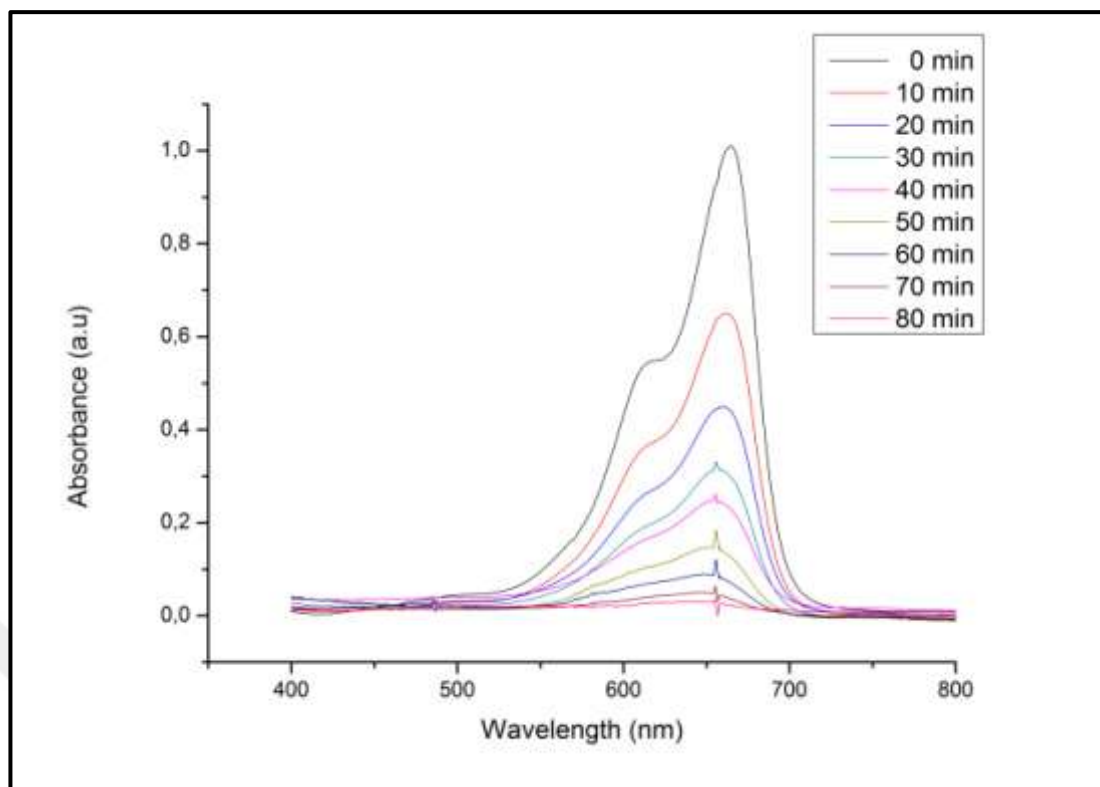


**Figure 3.9** Photocatalytic removal of methylene blue under UV light exposure by using 10 mg ZnO nanoparticles as catalyst.

Maximum 98.5 % decolorization was obtained at the end of the 80 min UV light exposure. The percent dye removal of ZnO nanoparticle is given in Table 3.1.

**Table 3.1** Percent dye removal efficiency of ZnO nanoparticle under UV light exposure.

<b>Time (min)</b>	<b>% Removal (ZnO)</b>
0	
10	36.0
20	56.0
30	70.5
40	77.0
50	87.5
60	93.0
70	96.5
80	98.5
90	98.5

After that dye removal efficiency of PEDOT polymer was checked as a reference photocatalyst to make comparison with main catalyst  $\text{SiO}_2\text{-CoFe}_2\text{O}_4\text{/PEDOT/ZnO}$  nanocomposite material. Results are given in Figure 3.10 and Table 3.2.

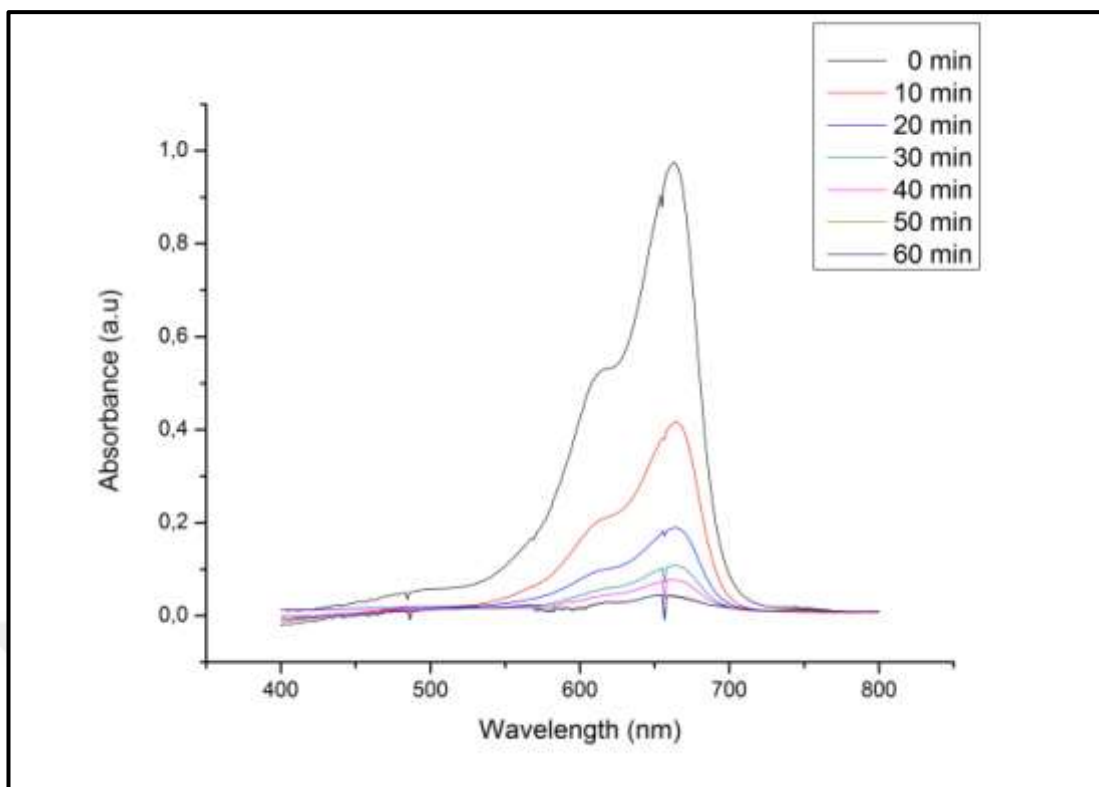


**Figure 3.10** Photocatalytic removal of methylene blue under UV light exposure by using 10 mg PEDOT as catalyst.

**Table 3.2** Percent dye removal efficiency of PEDOT polymer under UV light exposure.

<b>Time (min)</b>	<b>% Removal (PEDOT)</b>
0	
10	57.0
20	80.5
30	89.0
40	91.0
50	94.5
60	95.0
70	95.0

As can be seen from the results, 95.0 % removal of MB was obtained after 60 min with the usage of PEDOT polymer as a photocatalysts under UV light radiation. As can be seen that from Table 3.4 and 3.5, the percent removals for different durations, the initial MB removal rate of the PEDOT as photocatalyst is higher than the initial rate of ZnO nanoparticle used as photocatalyst.

After that photocatalytic removal of methylene blue under UV light irradiation in the presence of 10 mg PEDOT/ZnO nanocomposite material was checked. The results are given in Figure 3.11 and Table 3.3.

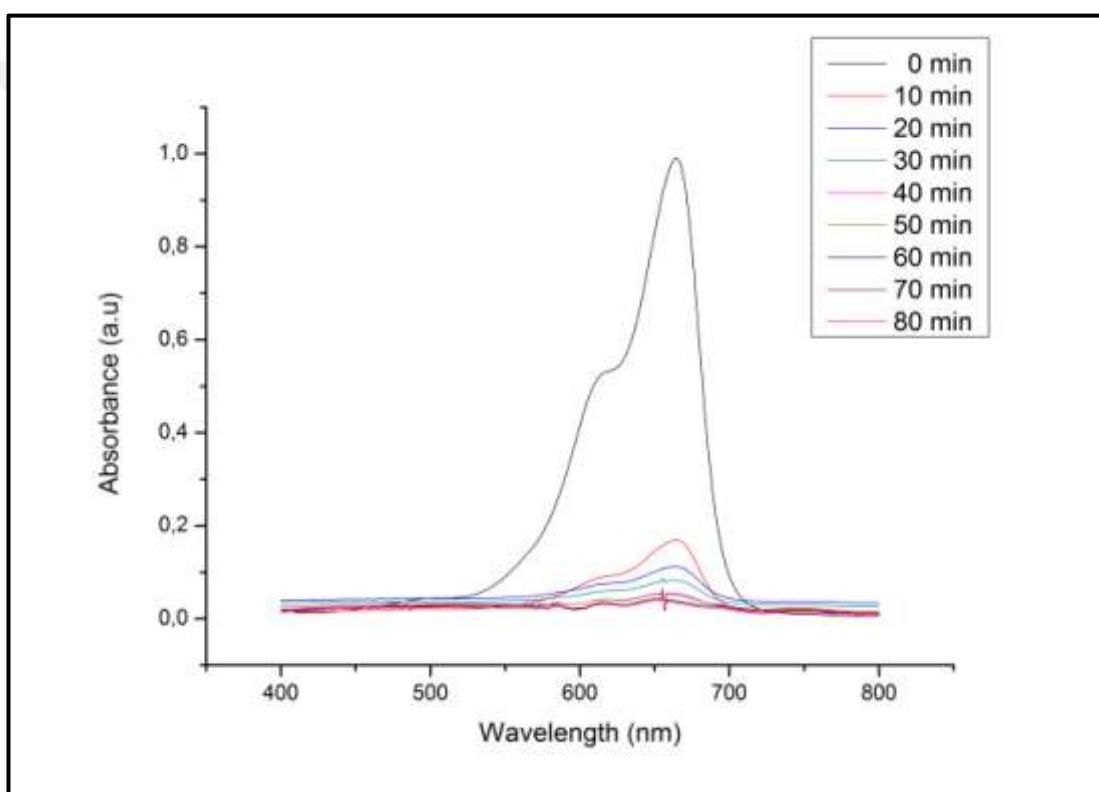


**Figure 3.11** Photocatalytic removal of methylene blue under UV light exposure by using 10 mg PEDOT/ZnO nanocomposite material as catalyst.

**Table 3.3** Percent dye removal efficiency of PEDOT/ZnO nanocomposite material under UV light exposure.

<b>Time (min)</b>	<b>% Removal (PEDOT-ZnO)</b>
0	
10	83.0
20	89.0
30	91.5
40	94.0
50	96.5
60	98.0
70	98.5
80	98.5

As can be seen from the Table 3.3, almost the total decolorization of MB was obtained at the end of the 60 min. UV light radiation. Thus, improved catalytic activity was obtained with the usage of the PEDOT/ZnO nanocomposite material as photocatalyst when compared with the results obtained with ZnO nanoparticles and PEDOT as photocatalyst.

Finally photocatalytic decolorization of methylene blue under UV light irradiation in the presence of 10 mg SiO<sub>2</sub>-CoFe<sub>2</sub>O<sub>4</sub>/PEDOT/ZnO nanocomposite material was checked under UV light exposure at different time intervals. The results are given in Figure 3.12 and Table 3.4.

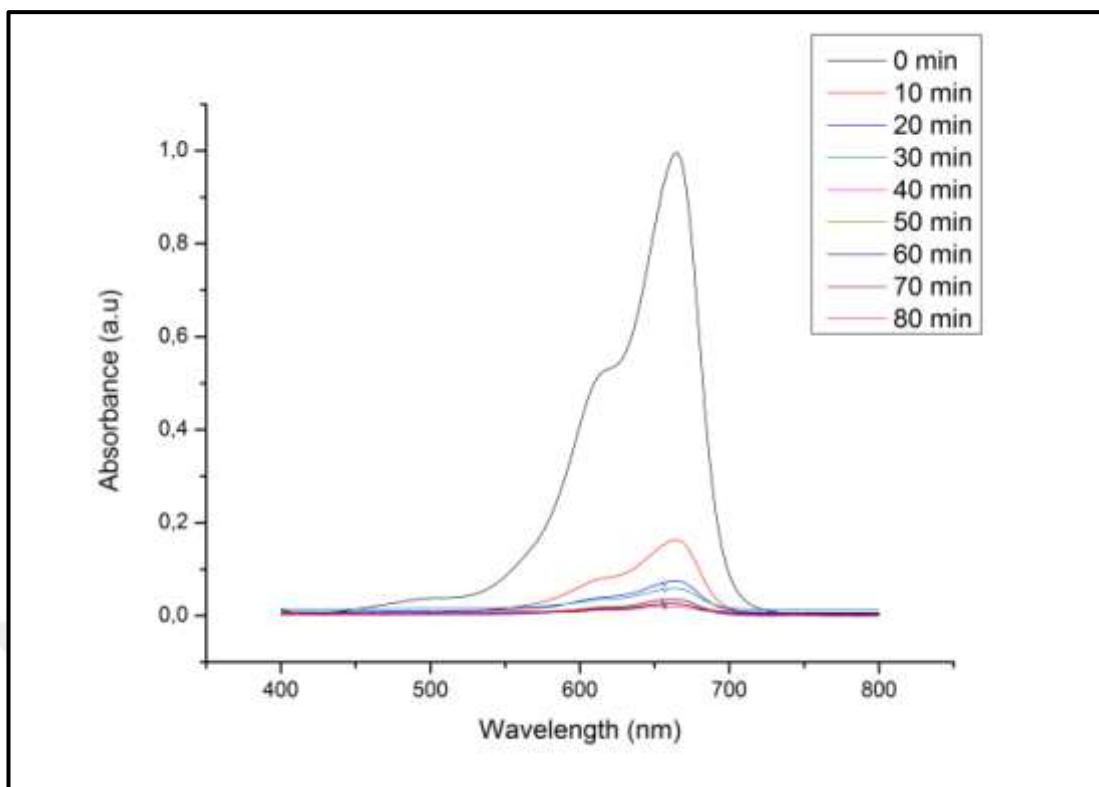


**Figure 3.12** Photocatalytic removal of methylene blue under UV light exposure by using 10 mg SiO<sub>2</sub>-CoFe<sub>2</sub>O<sub>4</sub>/PEDOT/ZnO nanocomposite material as catalyst.

**Table 3.4** Percent dye removal efficiency of SiO<sub>2</sub>-CoFe<sub>2</sub>O<sub>4</sub>/PEDOT/ZnO nanocomposite material under UV light exposure.

Time (min)	% Removal (MNPs-PEDOT- ZnO)
0	
10	84.0
20	92.5
30	94.5
40	97.0
50	98.5
60	99.0
70	99.0
80	99.0

As can be seen from the Table 3.4 highest catalytic activity was observed with the usage of SiO<sub>2</sub>-CoFe<sub>2</sub>O<sub>4</sub>/PEDOT/ZnO nanocomposite material as photocatalyst. The highest degradation efficiency was obtained as 84.0 % in 10 min. by using SiO<sub>2</sub>-CoFe<sub>2</sub>O<sub>4</sub>/PEDOT/ZnO nanocomposite material. Total decolorization of MB was obtained in 40 min. by using same conditions with the previous photocatalysts. In all experiments 10 mg catalyst was used. In the case of SiO<sub>2</sub>-CoFe<sub>2</sub>O<sub>4</sub>/PEDOT/ZnO 10 mg nanocomposite material contains nearly 2 mg ZnO nanoparticles and 3 mg PEDOT polymer.

Despite the less amount usage, improved catalytic activity was obtained due to synergetic effect obtained between ZnO nanoparticles and PEDOT polymer. Besides, the nano nature of the magnetic nanoparticles helps the increase of the surface area of the resulting catalyst which increases the number of active sides. So the SiO<sub>2</sub>-CoFe<sub>2</sub>O<sub>4</sub>/PEDOT/ZnO nanocomposite material prepared with the proposed facile method shows remarkable catalytic activity than the ZnO nanoparticles and PEDOT polymer.

In addition to improved catalytic activity, prepared SiO<sub>2</sub>-CoFe<sub>2</sub>O<sub>4</sub>/PEDOT/ZnO nanocomposite material has magnetic separation property which allows the easy removal of photocatalyst from the reaction medium at the end of the process by using external magnetic field.

## **CHAPTER 4**

### **CONCLUSION**

Semiconductor photocatalysts, recently, are one of the crucial wastewater treatments to eliminate several pollutants due to impressive qualities, such as nontoxic, superior electronic property, relatively inexpensive, and proper stability depending on heat and chemically. Yet, there are some fundamental disadvantages of semiconductors that affect the application of them adversely for photocatalytic processes. For example, separation and recycling of the conventional semiconductor photocatalysts from photocatalytic system possess difficulties that limit their application. In other words, discarding tiny semiconductor particles from huge amount of water requires great effort and further cost. To overcome such disadvantages, magnetic nanoparticles are joined to the structure as a carrier to enhance recycling efficiency, so that the photocatalyst can easily be collected via a magnet. The magnetic core provides the recovering of submicron sized photocatalyst from waste water by using powerful external magnetic field properly. By the way, the direct coating of magnetic nanoparticles to the surface of semiconductor causes the decrease in the activity of photocatalyst nanomaterial, because magnetic core results in the recombination of photogenerated electron and holes as being recombination center, thus results in the formation of less active species. For this reason different approaches are needed to increase the catalytic activity by doping semiconductor material for protection of the direct interaction of magnetic nanoparticles and semiconductors.

As a conclusion, PEDOT modified  $\text{SiO}_2\text{-CoFe}_2\text{O}_4$  magnetic nanoparticle added ZnO ( $\text{SiO}_2\text{-CoFe}_2\text{O}_4\text{/PEDOT/ZnO}$ ) nanocomposite materials were synthesized via in situ polymerization method. The  $\text{SiO}_2\text{-CoFe}_2\text{O}_4\text{/PEDOT/ZnO}$  nanocomposite materials exhibit improved catalytic activity during degradation reaction of MB dye solution under UV light exposure. The degradation process of MB solution was completed in 50 min by using prepared photocatalyst. The improved catalytic activity of  $\text{SiO}_2\text{-CoFe}_2\text{O}_4\text{/PEDOT/ZnO}$  nanocomposite material was observed that is related with the synergistic effect between PEDOT and ZnO nanoparticles and increased surface area with the addition of magnetic nanoparticles which increases the number of active sites. The presence of PEDOT polymer increases the activity by doping effect and also protection of semiconductors from the direct interaction with magnetic nanoparticles. The prepared nanocomposite photocatalyst has magnetic property so that it can easily be collected and separated from water by using external magnetic field. For this reason,  $\text{SiO}_2\text{-CoFe}_2\text{O}_4\text{/PEDOT/ZnO}$  nanocomposites are suitable candidates for photocatalytic treatment of wastewater.

## REFERENCES

1. Cooper, P. (1993). Removing colour from dyehouse waste waters—a critical review of technology available. *Coloration Technology*, 109(3), 97-100.
2. Chen, D., Sivakumar, M., & Ray, A. K. (2000). Heterogeneous photocatalysis in environmental remediation. *Asia-Pacific Journal of Chemical Engineering*, 8(5-6), 505-550.
3. S .Bagheri & N.M .Julkapl. (2016) Environmental remediation pollutants. (2015).A review *International Journal of Inorganic Chemistry*, 36(3), 1-16.
4. Ullah, I., Ali, S., Hanif, M. A., & Shahid, S. A. (2012). Nanoscience for environmental remediation: a review. *International Journal of Chemical and Biochemical Sciences*, 2(1), 60-77.
5. Bolong, N., Ismail, A. F., Salim, M. R., & Matsuura, T. (2009). A review of the effects of emerging contaminants in wastewater and options for their removal. *Desalination*, 239(1-3), 229-246
6. Ziolli, R. L., & Jardim, W. F. (1998). Mechanism reactions of photodegradation of organic compounds catalyzed by TiO<sub>2</sub>. *Química Nova*, 21(3), 319-325.
7. Palmisano, G., Augugliaro, V., Pagliaro, M., & Palmisano, L. (2007). Photocatalysis: a promising route for 21<sup>st</sup> century organic chemistry. *Chemical Communications*, (33), 3425-3437.

8. Machado, A. E., França, M. D., Velani, V., Magnino, G. A., Velani, H. M., Freitas, F. S., & Schmücker, M. (2008). Characterization and evaluation of the efficiency of TiO<sub>2</sub>/zinc phthalocyanine nanocomposites as photocatalysts for wastewater treatment using solar irradiation. *International Journal of Photoenergy*, 2008, 1-12.
9. Nogueira, R. F., & Jardim, W. F. (1998). Heterogeneous Photocatalysis and Its Environmental Applications [a Fotocatálise Heterogênea E Sua Aplicação Ambiental]. *Química Nova*, 21, 69-72.
10. Kumar, S. G., & Devi, L. G. (2011). Review on modified TiO<sub>2</sub> photocatalysis under UV/visible light: selected results and related mechanisms on interfacial charge carrier transfer dynamics. *The Journal of Physical Chemistry A*, 115(46), 13211-13241.
11. Andreozzi, R., Caprio, V., Insola, A., & Marotta, R. (1999). Advanced oxidation processes (AOP) for water purification and recovery. *Catalysis Today*, 53(1), 51-59.
12. Fujishima, A., Zhang, X., & Tryk, D. A. (2007). Heterogeneous photocatalysis: from water photolysis to applications in environmental cleanup. *International Journal of Hydrogen Energy*, 32(14), 2664-2672.
13. Zinatloo-Ajabshir, S., Salavati-Niasari, M., & Hamadianian, M. (2015). Praseodymium oxide nanostructures: novel solvent-less preparation, characterization and investigation of their optical and photocatalytic properties. *RSC Advances*, 5(43), 33792-33800.
14. Mortazavi-Derazkola, S., Zinatloo-Ajabshir, S., & Salavati-Niasari, M. (2015). Preparation and characterization of Nd<sub>2</sub>O<sub>3</sub> nanostructures via a new facile solvent-less route. *Journal of Materials Science: Materials in Electronics*, 26(8), 5658-5667.
15. Fujishima, A., & Honda, K. (1972). Electrochemical photolysis of water at a semiconductor electrode. *Nature*, 238(5358), 37-38.

16. Hoffmann, M. R., Martin, S. T., Choi, W., & Bahnemann, D. W. (1995). Environmental applications of semiconductor photocatalysis. *Chemical Reviews*, 95(1), 69-96.
17. Khataee, A. R., Zarei, M., & Ordikhani-Seyedlar, R. (2011). Heterogeneous photocatalysis of a dye solution using supported TiO<sub>2</sub> nanoparticles combined with homogeneous photoelectrochemical process: Molecular degradation products. *Journal of Molecular Catalysis A: Chemical*, 338(1), 84-91.
18. Xiong, L., Sun, W., Yang, Y., Chen, C., & Ni, J. (2011). Heterogeneous photocatalysis of methylene blue over titanate nanotubes: Effect of adsorption. *Journal of Colloid and Interface Science*, 356(1), 211-216.
19. Houas, A., Lachheb, H., Ksibi, M., Elaloui, E., Guillard, C., & Herrmann, J. M. (2001). Photocatalytic degradation pathway of methylene blue in water. *Applied Catalysis B: Environmental*, 31(2), 145-157.
20. Ollis, D. F., Pelizzetti, E., & Serpone, N. (1991). Photocatalyzed destruction of water contaminants. *Environmental Science & Technology*, 25(9), 1522-1529.
21. Zhu, X., Yuan, C., Bao, Y., Yang, J., & Wu, Y. (2005). Photocatalytic degradation of pesticide pyridaben on TiO<sub>2</sub> particles. *Journal of Molecular Catalysis A: Chemical*, 229(1), 95-105.
22. Wei, L., Shifu, C., Wei, Z., & Sujuan, Z. (2009). Titanium dioxide mediated photocatalytic degradation of methamidophos in aqueous phase. *Journal of Hazardous Materials*, 164(1), 154-160
23. Yu, B., Zeng, J., Gong, L., Zhang, M., Zhang, L., & Chen, X. (2007). Investigation of the photocatalytic degradation of organochlorine pesticides on a nano-TiO<sub>2</sub> coated film. *Talanta*, 72(5), 1667-1674.

24. Vinu, R., & Madras, G. (2011). Photocatalytic degradation of water pollutants using nano-TiO<sub>2</sub>. *Energy Efficiency and Renewable Energy Through Nanotechnology* (pp. 625-677). Springer London.
25. Chatzitakis, A., Berberidou, C., Paspaltsis, I., Kyriakou, G., Sklaviadis, T., & Poullos, I. (2008). Photocatalytic degradation and drug activity reduction of chloramphenicol. *Water Research*, *42*(1), 386-394.
26. An, T., Yang, H., Li, G., Song, W., Cooper, W. J., & Nie, X. (2010). Kinetics and mechanism of advanced oxidation processes (AOPs) in degradation of ciprofloxacin in water. *Applied Catalysis B: Environmental*, *94*(3), 288-294.
27. Shah, S. I., Li, W., Huang, C. P., Jung, O., & Ni, C. (2002). Study of Nd<sup>3+</sup>, Pd<sup>2+</sup>, Pt<sup>4+</sup>, and Fe<sup>3+</sup> dopant effect on photoreactivity of TiO<sub>2</sub> nanoparticles. *Proceedings of the National Academy of Sciences*, *99*(suppl 2), 6482-6486.
28. Dvoranová, D., Brezová, V., Mazúr, M., & Malati, M. A. (2002). Investigations of metal-doped titanium dioxide photocatalysts. *Applied Catalysis B: Environmental*, *37*(2), 91-105.
29. Nagaveni, K., Hegde, M. S., & Madras, G. (2004). Structure and photocatalytic activity of Ti<sub>1-x</sub>M<sub>x</sub>O<sub>2±δ</sub> (M= W, V, Ce, Zr, Fe, and Cu) synthesized by solution combustion method. *The Journal of Physical Chemistry B*, *108*(52), 20204-20212.
30. Vinu, R., & Madras, G. (2009). Photocatalytic activity of Ag-substituted and impregnated nano-TiO<sub>2</sub>. *Applied Catalysis A: General*, *366*(1), 130-140.
31. Liu, G., Wang, L., Yang, H. G., Cheng, H. M., & Lu, G. Q. M. (2010). Titania-based photocatalysts—crystal growth, doping and heterostructuring. *Journal of Materials Chemistry*, *20*(5), 831-843.

32. Kuznetsov, V. N., & Serpone, N. (2006). Visible light absorption by various titanium dioxide specimens. *The Journal of Physical Chemistry B*, *110*(50), 25203-25209.
33. Brahim, R., Bessekhoad, Y., Bouguelia, A., & Trari, M. (2008). Improvement of eosin visible light degradation using PbS-sensitized TiO<sub>2</sub>. *Journal of Photochemistry and Photobiology A: Chemistry*, *194*(2), 173-180.
34. Kim, W., Park, J., Jo, H. J., Kim, H. J., & Choi, W. (2008). Visible light photocatalysts based on homogeneous and heterogenized tin porphyrins. *The Journal of Physical Chemistry C*, *112*(2), 491-499.
35. Georgekutty, R., Seery, M. K., & Pillai, S. C. (2008). A highly efficient Ag-ZnO photocatalyst: synthesis, properties, and mechanism. *The Journal of Physical Chemistry C*, *112*, 13563–13570.
36. Qiu, R., Zhang, D., Mo, Y., Song, L., Brewer, E., Huang, X., & Xiong, Y. (2008). Photocatalytic activity of polymer-modified ZnO under visible light irradiation. *Journal of Hazardous Materials*, *156*(1), 80-85.
37. Jiang, R., Zhu, H., Li, X., & Xiao, L. (2009). Visible light photocatalytic decolourization of CI Acid Red 66 by chitosan capped CdS composite nanoparticles. *Chemical Engineering Journal*, *152*(2), 537-542.
38. Muruganandham, M., & Kusumoto, Y. (2009). Synthesis of N, C codoped hierarchical porous microsphere ZnS as a visible light-responsive photocatalyst. *The Journal of Physical Chemistry C*, *113*(36), 16144-16150.
39. Miyauchi, M., Nakajima, A., Watanabe, T., & Hashimoto, K. (2002). Photocatalysis and photoinduced hydrophilicity of various metal oxide thin films. *Chemistry of Materials*, *14*(6), 2812-2816.

40. Akyol, A., & Bayramoğlu, M. (2005). Photocatalytic degradation of Remazol Red F<sub>3</sub>B using ZnO catalyst. *Journal of Hazardous Materials*, 124(1), 241-246.
41. Daneshvar, N., Salari, D., & Khataee, A. R. (2004). Photocatalytic degradation of azo dye acid red 14 in water on ZnO as an alternative catalyst to TiO<sub>2</sub>. *Journal of Photochemistry and Photobiology A: Chemistry*, 162(2), 317-322.
42. Su, S., Lu, S. X., & Xu, W. G. (2008). Photocatalytic degradation of reactive brilliant blue X-BR in aqueous solution using quantum-sized ZnO. *Materials Research Bulletin*, 43(8), 2172-2178.
43. Lu, C., Wu, Y., Mai, F., Chung, W., Wu, C., Lin, W., & Chen, C. (2009). Degradation efficiencies and mechanisms of the ZnO-mediated photocatalytic degradation of Basic Blue 11 under visible light irradiation. *Journal of Molecular Catalysis A: Chemical*, 310(1), 159-165.
44. Kansal, S. K., Ali, A. H., & Kapoor, S. (2010). Photocatalytic decolorization of biebrich scarlet dye in aqueous phase using different nanophotocatalysts. *Desalination*, 259(1), 147-155.
45. Khodja, A. A., Sehili, T., Pilichowski, J. F., & Boule, P. (2001). Photocatalytic degradation of 2-phenylphenol on TiO<sub>2</sub> and ZnO in aqueous suspensions. *Journal of Photochemistry and Photobiology A: Chemistry*, 141(2), 231-239.
46. Colón, G., Hidalgo, M. C., Navío, J. A., Melián, E. P., Díaz, O. G., & Rodríguez, J. D. (2008). Highly photoactive ZnO by amine capping-assisted hydrothermal treatment. *Applied Catalysis B: Environmental*, 83(1), 30-38.
47. Evgenidou, E., Konstantinou, I., Fytianos, K., Poullos, I., & Albanis, T. (2007). Photocatalytic oxidation of methyl parathion over TiO<sub>2</sub> and ZnO suspensions. *Catalysis Today*, 124(3), 156-162.

48. Aal, A. A., Mahmoud, S. A., & Aboul-Gheit, A. K. (2009). Sol-gel and thermally evaporated nanostructured thin ZnO films for photocatalytic degradation of trichlorophenol. *Nanoscale Research Letters*, 4(7), 627.
49. Chen, C. C. (2007). Degradation pathways of ethyl violet by photocatalytic reaction with ZnO dispersions. *Journal of Molecular Catalysis A: Chemical*, 264(1), 82-92.
50. Kandavelu, V., Kastien, H., & Thampi, K. R. (2004). Photocatalytic degradation of isothiazolin-3-ones in water and emulsion paints containing nanocrystalline TiO<sub>2</sub> and ZnO catalysts. *Applied Catalysis B: Environmental*, 48(2), 101-111.
51. Domenech, J., & Prieto, A. (1986). Stability of zinc oxide particles in aqueous suspensions under UV illumination. *The Journal of Physical Chemistry*, 90(6), 1123-1126.
52. Kislov, N., Lahiri, J., Verma, H., Goswami, D. Y., Stefanakos, E., & Batzill, M. (2009). Photocatalytic degradation of methyl orange over single crystalline ZnO: orientation dependence of photoactivity and photostability of ZnO. *Langmuir*, 25(5), 3310-3315.
53. Pare, B., Jonnalagadda, S. B., Tomar, H., Singh, P., & Bhagwat, V. W. (2008). ZnO assisted photocatalytic degradation of acridine orange in aqueous solution using visible irradiation. *Desalination*, 232(1), 80-90.
54. Sakthivel, S., Neppolian, B., Shankar, M. V., Arabindoo, B., Palanichamy, M., & Murugesan, V. (2003). Solar photocatalytic degradation of azo dye: comparison of photocatalytic efficiency of ZnO and TiO<sub>2</sub>. *Solar Energy Materials and Solar Cells*, 77(1), 65-82.
55. Dindar, B., & Içli, S. (2001). Unusual photoreactivity of zinc oxide irradiated by concentrated sunlight. *Journal of Photochemistry and Photobiology A: Chemistry*, 140(3), 263-268.

56. Pardeshi, S. K., & Patil, A. B. (2008). A simple route for photocatalytic degradation of phenol in aqueous zinc oxide suspension using solar energy. *Solar Energy*, 82(8), 700-705.
57. Sobana, N., & Swaminathan, M. (2007). Combination effect of ZnO and activated carbon for solar assisted photocatalytic degradation of Direct Blue 53. *Solar Energy Materials and Solar Cells*, 91(8), 727-734.
58. Comparelli, R., Fanizza, E., Curri, M. L., Cozzoli, P. D., Mascolo, G., & Agostiano, A. (2005). UV-induced photocatalytic degradation of azo dyes by organic-capped ZnO nanocrystals immobilized onto substrates. *Applied Catalysis B: Environmental*, 60(1), 1-11.
59. Zhang, L., Cheng, H., Zong, R., & Zhu, Y. (2009). Photocorrosion suppression of ZnO nanoparticles via hybridization with graphite-like carbon and enhanced photocatalytic activity. *The Journal of Physical Chemistry C*, 113(6), 2368-2374.
60. Zhang, H., Zong, R., & Zhu, Y. (2009). Photocorrosion inhibition and photoactivity enhancement for zinc oxide via hybridization with monolayer polyaniline. *The Journal of Physical Chemistry C*, 113(11), 4605-4611.
61. Lichtin, N. N., Avudaithai, M., Berman, E., & Grayfer, A. (1996). TiO<sub>2</sub>-photocatalyzed oxidative degradation of binary mixtures of vaporized organic compounds. *Solar Energy*, 56(5), 377-385.
62. Daniele, S., Ghazzal, M. N., Hubert-Pfalzgraf, L. G., Duchamp, C., Guillard, C., & Ledoux, G. (2006). Preparations of nano-particles, nano-composites and fibers of ZnO from an amide precursor: Photocatalytic decomposition of (CH<sub>3</sub>)<sub>2</sub>S<sub>2</sub> in a continuous flow reactor. *Materials Research Bulletin*, 41(12), 2210-2218.
63. El-Kemary, M., El-Shamy, H., & El-Mehasseb, I. (2010). Photocatalytic degradation of ciprofloxacin drug in water using ZnO nanoparticles. *Journal of Luminescence*, 130(12), 2327-2331.

64. Velmurugan, R., & Swaminathan, M. (2011). An efficient nanostructured ZnO for dye sensitized degradation of Reactive Red 120 dye under solar light. *Solar Energy Materials and Solar Cells*, 95(3), 942-950.
65. Kitture, R., Koppikar, S. J., Kaul-Ghanekar, R., & Kale, S. N. (2011). Catalyst efficiency, photostability and reusability study of ZnO nanoparticles in visible light for dye degradation. *Journal of Physics and Chemistry of Solids*, 72(1), 60-66.
66. Shinde, V. R., Gujar, T. P., Noda, T., Fujita, D., Vinu, A., Grandcolas, M., & Ye, J. (2010). Growth of shape-and size-selective zinc oxide nanorods by a microwave-assisted chemical bath deposition method: Effect on photocatalysis properties. *Chemistry-A European Journal*, 16(34), 10569-10575.
67. Xu, F., Zhang, P., Navrotsky, A., Yuan, Z. Y., Ren, T. Z., Halasa, M., & Su, B. L. (2007). Hierarchically assembled porous ZnO nanoparticles: synthesis, surface energy, and photocatalytic activity. *Chemistry of Materials*, 19(23), 5680-5686.
68. Li, X., Lv, K., Deng, K., Tang, J., Su, R., Sun, J., & Chen, L. (2009). Synthesis and characterization of ZnO and TiO<sub>2</sub> hollow spheres with enhanced photoreactivity. *Materials Science and Engineering: B*, 158(1), 40-47.
69. Li, X., Lv, K., Deng, K., Tang, J., Su, R., Sun, J., & Chen, L. (2009). Synthesis and characterization of ZnO and TiO<sub>2</sub> hollow spheres with enhanced photoreactivity. *Materials Science and Engineering: B*, 158(1), 40-47.
70. Wang, Y., Li, X., Wang, N., Quan, X., & Chen, Y. (2008). Controllable synthesis of ZnO nanoflowers and their morphology-dependent photocatalytic activities. *Separation and Purification Technology*, 62(3), 727-732.
71. B. Li, Y. Wang, (2009). Facile synthesis and enhanced photocatalytic performance of flower-like ZnO hierarchical microstructures, *The Journal of Physical Chemistry C*, 114, 890–896.

72. Subramanian, V., Wolf, E. E., & Kamat, P. V. (2003). Green emission to probe photoinduced charging events in ZnO– Au nanoparticles. Charge distribution and Fermi-level equilibration. *The Journal of Physical Chemistry B*, *107*(30), 7479-7485.
73. Wu, J. J., & Tseng, C. H. (2006). Photocatalytic properties of nc-Au/ZnO nanorod composites. *Applied Catalysis B: Environmental*, *66*(1), 51-57.
74. Height, M. J., Pratsinis, S. E., Mekasuwandumrong, O., & Praserthdam, P. (2006). Ag-ZnO catalysts for UV-photodegradation of methylene blue. *Applied Catalysis B: Environmental*, *63*(3), 305-312.
75. Li, B., & Cao, H. (2011). ZnO@ graphene composite with enhanced performance for the removal of dye from water. *Journal of Materials Chemistry*, *21*(10), 3346-3349.
76. Kamegawa, D. Yamahana & H. Yamashita .(2010) .Graphene coating of TiO<sub>2</sub> nanoparticles *The Journal of Physical Chemistry C*, *114* (35), 15049–15053.
77. Ma, D., Aguiar, M., Freire, J. A., & Hümmelgen, I. A. (2000). Organic reversible switching devices for memory applications. *Advanced Materials*, *12*(14), 1063-1066.
78. Chowdhury, D., Paul, A., & Chattopadhyay, A. (2005). Photocatalytic polypyrrole– TiO<sub>2</sub>– nanoparticles composite thin film generated at the air– water interface. *Langmuir*, *21*(9), 4123-4128.
79. Cho, S., & Choi, W. (2001). Solid-phase photocatalytic degradation of PVC– TiO<sub>2</sub> polymer composites. *Journal of Photochemistry and Photobiology A: Chemistry*, *143*(2), 221-228.
80. Mills, G., & Hoffmann, M. R. (1993). Photocatalytic degradation of pentachlorophenol on titanium dioxide particles: identification of intermediates and mechanism of reaction. *Environmental Science & Technology*, *27*(8), 1681-1689.

81. Kormann, C., Bahnemann, D. W., & Hoffmann, M. R. (1991). Photolysis of chloroform and other organic molecules in aqueous titanium dioxide suspensions. *Environmental Science & Technology*, 25(3), 494-500.
82. Carraway, E. R., Hoffman, A. J., & Hoffmann, M. R. (1994). Photocatalytic oxidation of organic acids on quantum-sized semiconductor colloids. *Environmental Science & Technology*, 28(5), 786-793.
83. Hoffmann, M. R., Martin, S. T., Choi, W., & Bahnemann, D. W. (1995). Environmental applications of semiconductor photocatalysis. *Chemical Reviews*, 95(1), 69-96.
84. Groenendaal, L., Jonas, F., Freitag, D., Pielartzik, H., & Reynolds, J. R. (2000). Poly (3, 4-ethylenedioxythiophene) and its derivatives: past, present, and future. *Advanced Materials*, 12(7), 481-494.
85. Roncali, J., Blanchard, P., & Frère, P. (2005). 3, 4-Ethylenedioxythiophene (EDOT) as a versatile building block for advanced functional  $\pi$ -conjugated systems. *Journal of Materials Chemistry*, 15(16), 1589-1610.
86. Kumar, A., Buyukmumcu, Z., & Sotzing, G. A. (2006). Poly (thieno [3, 4-b] furan). A new low band gap conjugated polymer. *Macromolecules*, 39(8), 2723-2725.
87. Biallozor, S., Kupniewska, A., & Jasulajtenea, V. (2004). Properties of electrodes modified with poly (3, 4-ethylenedioxythiophene) and Pt particles- Part I. *Bulletin of Electrochemistry*, 20(5), 231-236.
88. Niu, L., Li, Q., Wei, F., Chen, X., & Wang, H. (2003). Formation optimization of platinum-modified polyaniline films for the electrocatalytic oxidation of methanol. *Synthetic Metals*, 139(2), 271-276.

89. Sclafani, A., Palmisano, L., & Schiavello, M. (1990). Influence of the preparation methods of titanium dioxide on the photocatalytic degradation of phenol in aqueous dispersion. *Journal of Physical Chemistry*, 94(2), 829-832.
90. Sato, J., Kobayashi, H., Ikarashi, K., Saito, N., Nishiyama, H., & Inoue, Y. (2004). Photocatalytic activity for water decomposition of RuO<sub>2</sub>-dispersed Zn<sub>2</sub>GeO<sub>4</sub> with d10 configuration. *The Journal of Physical Chemistry B*, 108(14), 4369-4375.
91. Matsuoka, M., & Anpo, M. (2003). Local structures, excited states, and photocatalytic reactivities of highly dispersed catalysts constructed within zeolites. *Journal of Photochemistry and Photobiology C: Photochemistry Reviews*, 3(3), 225-252.
92. Zinatloo-Ajabshir, S., Salavati-Niasari, M., & Hamadani, M. (2015). Praseodymium oxide nanostructures: novel solvent-less preparation, characterization and investigation of their optical and photocatalytic properties. *RSC Advances*, 5(43), 33792-33800.
93. David, G., Fundueanu, G., Pinteala, M., Minea, B., Dascalu, A., & Simionescu, B. C. (2014). Polymer engineering for drug/gene delivery: from simple towards complex architectures and hybrid materials. *Pure and Applied Chemistry*, 86(11), 1621-1635.
94. Stöber, W., Fink, A., & Bohn, E. (1968). Controlled growth of monodisperse silica spheres in the micron size range. *Journal of Colloid and Interface Science*, 26(1), 62-69.